RADON PROGENY DEPOSITION IN RESPIRATORY TRACT: COMPARATIVE ANALYSIS OF MODELS

By

Tamiru Bayissa

A THESIS PRESENTED TO

THE SCHOOL OF GRADUATE STUDIES
ADDIS ABABA UNIVERSITY

IN PARTIAL FULFILLMENT OF THE REQUIREMENTS
FOR THE DEGREE

MASTER OF SCIENCE in PHYSICS

ADDIS ABABA, ETHIOPIA

JULY 2011

ADDIS ABABA UNIVERSITY
SCHOOL OF GRADUATE STUDIES

RADON PROGENY DEPOSITION IN RESPIRATORY TRACT: COMPARATIVE ANALYSIS OF MODELS

By
Tamiru Bayissa
Deaprment of Physics
Addis Ababa University

Approved by the Examining Board:

Dr. Tilahun Tesfaye (Ass. Professor)	Advisor	_____
Professor A.K. Chaubey	Examiner	_____
Professor Seetharami Reddy	Examiner	_____

Dated: July 2011

This Work is Dedicated to My Mother

Table of Contents

List of Tables

List of Figures

ACKNOWLEDGEMENTS

Above all, I would like to thank God, for letting me accomplish this stage. I would like to express my deepest gratitude and respect to my advisor Dr.Tilahun Tesfaye for his guidance, assistance, supervision and contribution of valuable suggestions throughout the whole period of the research work.

I would like also to thank mom who really feels my busyness and provides me all my requirements. Finally, I would like to thank MOE for financial support and thanks be to my friends for all kinds of encouragement and support I get from them.

Addis Ababa University

June, 2011

ABSTRACT

Cheng (2003) model of the extra-thoracic respiratory tract was used to calculate the deposition efficiency of aerosols of aerodynamic diameter ranging from 0.1μ m to 72μ m. The model assumes the deposition in the extra-thoracic region is mainly due to nasal airway geometry and the critical dimension is the minimum cross-sectional area in the nasal passage. A dimensionless Stokes number is calculated as a function of the the aerodynamic diameter (d_{a}), flow rate (Q), and the minimum cross-sectional area (A_{min}). Literature value of $A_{\mathrm{min}} = 1.61\,\mathrm{cm}^2$ was used in the calculation of Stokes number.

The calculation done using this model agrees with the predictions of the ICRP 1994 respiratory tract model. Further this model gives good agreement to the experimental results available in literature by introducing adjusting parameters for breathing rate and specific geometries of individuals.

CHAPTER 1
AEROSOLS AND RADON

1.1 RADON

Radon is odorless, tasteless and chemically inert gases. At standard temperature and pressure, it is colorless but at low temperature (as cooled below freezing) it has brilliant phosphorescence which turns yellow as temperature lowered and Orange red at the temperature air liquefies (Bemenet Alemayehu, 2006). It is soluble in organic liquids than water.

1.1.1 Origin and Concentration of Radon

Radon is a radioactive noble gas. It is the decay product of ^{226}Ra. ^{226}Ra is the sixth member of natural radioactive series of ^{238}U with half life 1620 years, it will decay in to radon by emission alpha particle. It found manly in soil and rocks and provide continuous source of ^{222}Rn (ICRP, 2009). As a result, radon is ubiquitous present every where but it's concentration vary from one location to another.

All radon isotopes are radioactive. However, 36 radioactive isotopes have been characterized with their atomic mass from 193 to 228. But the three naturally occurring isotopes are well known; ^{222}Rn the uranium series and the most stable isotopes with half life 3.8d. The second one is thoron (^{220}Rn) which is a member of Thorium series. The parent nuclide of Thoron,^{232}Th is more abundant than ^{238}U but it has longer half life as a result the average rate of production of ^{220}Rn in the ground is about the same as that of ^{222}Rn, however, the short half life ^{220}Rn, 56s. As compared with 3.8 d for ^{222}Rn gives it much greater chance to decay before becoming air borne. The contribution of the daughter of ^{220}Rn to lung dose are usually negligible compared with ^{222}Rn (Turner, 1995). The third one is derived from isotopes of actinium (^{227}Ac) is called actinon (^{219}Rn), it is alpha emitter with half life 3.96s. It′s concentration to air borne is insignificant because of relatively rare original nuclide^{235}U.

In open air radon concentration range from 1 to 100 Bqm^{-3}, even less than 0.1 Bqm^{-3}. This dose not significant radiation hazard. However, in cave or the area

of mines climb from 20 to 2000 Bqm^{-3} and in some closed space line in door environments ^{222}Rn is accumulated due to poor ventilation. The ^{222}Rn concentration can be reach a very high level in the source strength is large and the ventilation is poor high radon concentration in the door of a few hundred of Bqm^{-3} or more can represent significant radiation hazards (Yu et al., 2006).

Radon it self posses little health hazard because of it is inert gas not reactive but when it inhaled the potential health hazard arise. Radon decay in to non gaseous radio active daughters. When radon daughters trapped in the respiratory system they will decay before being removed by a normal lung clearing mechanism of a body. These daughters are non gaseous they will deposit in lung and they emit radiations. These emitted radiations damage the sensitive tissue and may cause lunge cancer. Some fraction of the radon progeny will also penetrate lunges in to the blood and irradiate the whole human body (Yu et al., 2006).

1.1.2 Health Hazards of Radon

Harmful effects of radon and its progeny are very well confirmed from underground uranium miners. There are several epidemiological studies that follow the health status of large populations of miners (Yu et al., 2006).

Radiation exposure is not limited only to miners. Every one is continually exposed to ionizing radiation which has always been present in the environment. Most of the radiation from naturally occurring sources such as radium in drinking water, ^{40}Ca in living tissue, the heavy radio active elements in rock, stone and cosmic rays. After 1895 man made sources added to these sources (Turner, 1995). The main naturally radio active active contaminate is ^{222}Rn has been established that about half of the total effective dose received by human bing from all source of the ionizing radiation is attributed to ^{222}Rn and its progeny (Yu et al., 2006) .

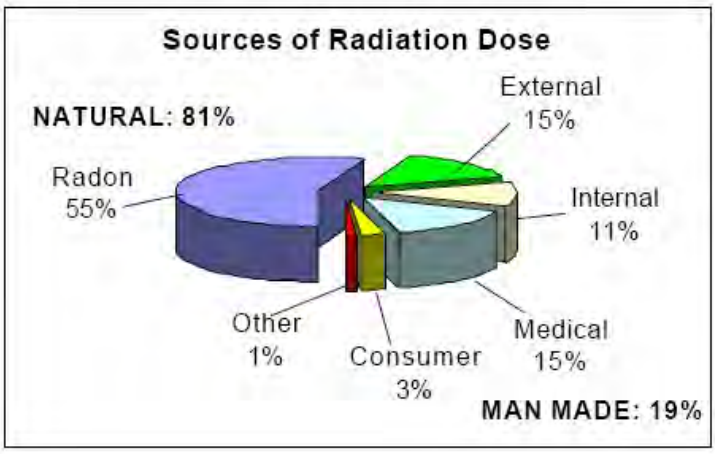

Figure 1.1: Dose received by human bing from all source of the ionizing radiation

The health hazard from radon is closely related to the air concentration of the potential of alpha particle energy of the short lived daughters. The concentration of the radon should be expressed with some quantities. There are several special physical quantities and units in the field of radon dosimetry (some of them listed in table 1.1). But concentration of radon progeny usually measured by the quantity called potential alpha energy concentration (PAEC) defined as total energy of alpha particles emitted by the radon progeny in a unit volume of undisturbed air. It calculated as:

$$PAEC = \sum_{i=1}^{4} C_i E_i \tag{1.1}$$

where C_i is the number of atoms i^{th} radon progeny in m^{-3} of air and E_i corresponding potential alpha energy in joule (J) PAEC can be expressed in Jm^{-3}; while the traditional and the still very commonly used unit is Working Level (WL): It is any combination of short lived radon decay products in one liter of air that will result in the ultimate emission of 1.3×10^5 Mev of potential alpha energy. This number was chosen because it is approximately the alpha energy released from the decay products in equilibrium with 100 pci of ^{222}Rn. That is 1.3×10^5 of alpha potential energy is emitted during radon decay to ^{210}Pb (which is stable) in one liter of air.

$$W_L = 1.3 \times 10^5 Mev/Lit = 130 Mev/cm^3 = 20.83 \mu J/m^3 \tag{1.2}$$

The exposure to radon progeny X is the product of the PAEC and the exposure time t expressed as:

$$X = PAEC \times t \tag{1.3}$$

It expressed in Jsm^{-3} the traditional unit in use is called Working Level Month (WLM). The cumulative exposure to an individual exposed at the short lived radon progeny concentration of a working level (WL) over a working month of 170 hours is defined as a working level month (WLM). The modern quantity for expressing concentration of radon decay products is the equilibrium equivalent concentration (EEC), which represents the concentration of ^{222}Rn in equilibrium with its decay products that would have the same potential alpha to multiply by 6.4×10^5 to obtain $Bqhm^{-3}$ (EEC). EEC calculated as:

$$EEC(^{222}Rn) = 0.105(^{218}Po) + 0.516(^{214}Pb) + 0.379(^{214}Bi) \tag{1.4}$$

$$EEC(^{220}Rn) = 0.91(^{212}Pb) + 0.087(^{212}Bi) \tag{1.5}$$

where ^{218}Po ^{214}Pb etc.,EEC are in Bq/m^3(UNSCEAR, 2006).

The exposure of the human body to ionizing radiation, including radiation from radon and it′s progeny, is characterized by the effective dose E, which is a weighted

absorbed dose. There are two kinds of weighting, namely, according to the type of radiation and according to the type of irradiated tissue. The effective dose is defined as:

$$E = \sum_T w_T \sum_R w_R D_R \tag{1.6}$$

where D_R is the mean absorbed dose in the organs or tissues irradiated by the radiation R, w_R is the radiation weighting factor that accounts for the differences among various types of radiation and w_T is the tissue weighting factor which takes into account the different sensitivities of various tissues in the human body to radiations. The tissue weighting factor for the human lung is w_L = 0.12. The SI unit for the effective dose is Sievert (Sv). The effective dose is not a measurable quantity and is a subject of calculations only. To calculate the effective dose, some models, called dosimetric models, are needed. In other words, a dosimetric model of the human respiratory tract is needed for dose calculations in the human lung.

One of the most important components of any Rn progeny dosimetry model is the deposition model, and the parameter values used in the calculations. Because aerosol deposition is so important for any inhaled materials.

Quantity	SI Unit	traditional Unit	conversion factor
Activity	becquerel(Bq)	curie(Ci)	1Ci = 3.7 $\times$ 10^{10} Bq
concentration	Bq/m^3	PCi/L	PCi/L = 37 Bq/m^3
PAEC	J/m^3	Working level (WL)	WL = 2.08 $\times$ 10^{-5} J/m^3
Exposure	Js/m^3	WLM	WLM = 12.97 Js/m^3
Exposure Rate	J/m^3	WLM/y	WLM/y = 4.11$\times$ 10^{-7} J/m^3

Table 1.1: Physical quantities and units relevant to Rn and Rn progeny (Johnson et al., 1991)

Determination of the effective dose in the human lung for a given exposure condition is a very complicated task. To enable the calculations dose due to radon and radon progeny (attached and unattached) one of the most important components of any Rn progeny dosimetry model is the deposition model, and the parameter values used in the calculations. Because aerosol deposition is so important for any inhaled material then one should know radon concentration in aerosol and deposition of aerosol in respiratory tract (Yu et al., 2006).

1.2 Aerosols

Solid or liquid disperse systems in a gas phase medium are referred to as aerosols. Aerosol refers to system of solid or liquid particle of sufficiently small diameter

to maintain stability as suspension in air as defined by Green and Lane (Stuart, 1984).

Aerosols are broadly classified as dispersion aerosols and condensation aerosols on the basis of their formation.

Dispersion aerosols are those formed by the grinding or atomization of solids and liquids followed by transfer of powders into a state of suspension.

Condensation aerosols are formed when supersaturated vapors condense and as a result of reaction between gases leading to the formation of no-volatile product such as soot.

Dusts are dispersion aerosols while smokes are condensation aerosols with a solid disperse phase. Mist and smog are aerosols containing both condensation and dispersion.

Aerosols may result from a natural phenomenon such as a fire or a volcano, or can be of anthropogenic origin from the burning of fossil fuels. Human activity accounts for approximately 10%, most of the 10% are from the northern hemisphere.

1.2.1 Size and Size Distribution of Aerosols

Aerosols are found in the air with varying size, type and concentration. Particles of radius less than 5nm have very short life time in air because they become attached to larger particles and can exist in a considerable concentration only if produced constantly. Reaction products, ions and decay products are examples of aerosols of size less than 5nm Junge (1963).

The size of aerosols in air ranges from clusters of few molecules to about 20nm radius. The upper limit of aerosol size is due to sedimentation, i.e., if the radius of a particle is more than about 20nm lasts only short time in air before it is deposited. Therefore atmospheric aerosols thus defined forms a spectrum which extends over almost four orders of magnitude. The concentration of aerosols in the air also a varied function of temperature, humidity, their size distribution and ventilation rate.

An aerosol is typically a micron in size. The lower size limit is a couple of nanometers, that is to say when the particles consist of single molecules. The higher limit is set to particle sizes around 100 μm, meaning that they can remain air borne for a couple of seconds.

Aerosols of sizes smaller than about 1 micron are mostly produced from smoke and soot or from condensation processes. Like SO_2 gas stemming from a volcano, which reacts to become sulphate particles. Aerosols of larger size are normally instigated from wind blown dust or salt in sea spray. In a typical cloud aerosol

sizes are about 10 microns or more. Most aerosols are suspended in the lower atmosphere called the troposphere. They remain here up to approximately a week, and are washed out by precipitation (ERNBO, 2006). Aerosols originating from volcanoes are transported with eruptive flows of gas into stratosphere. Aerosols in the stratosphere may remain for years while in the troposphere, precipitation and interactions with Earth′s surface remove aerosols in ten days or less (GLOBE, 2002).

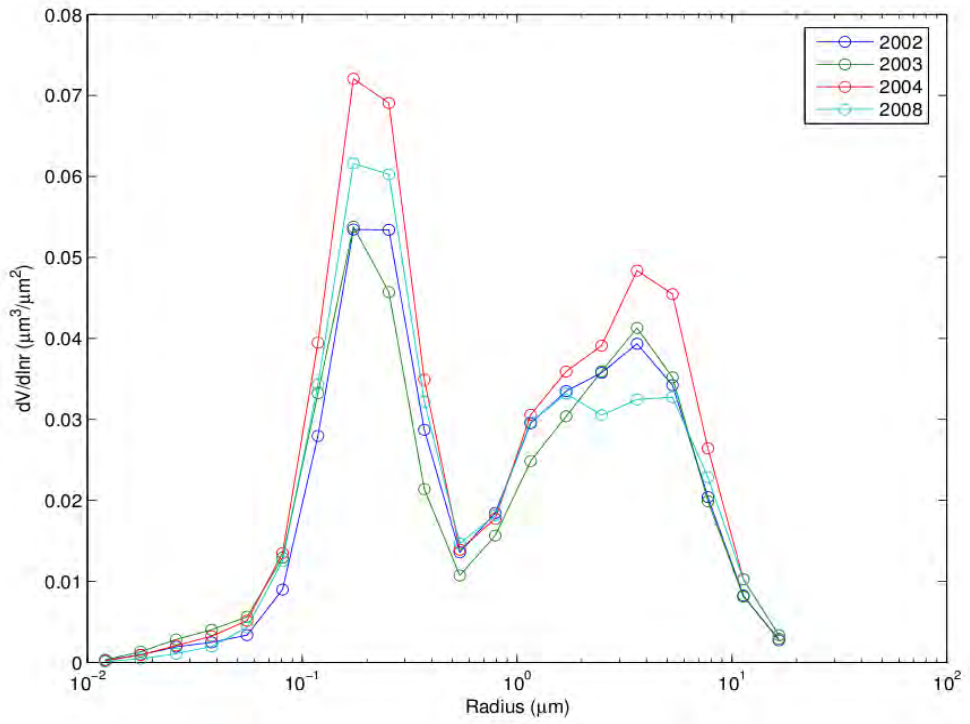

Figure 1.2: Average aerosol size distributions in 2002, 2003, 2004 and 2008 respectively in Hong Kong

(Yang & Wenig, 2009)

Aerosols are too small their size from 0.01 to 10 μm radii (Hobbs, 1993) to be individually visible, but you can often see their combined effect when the sky is hazy or looks dirty. Brilliant orange skies at sunrise and sunset may also be indicators that aerosols are present.

Aerosol concentration vary significantly with location and time. There are seasonal variations as well as unpredictable changes due to events such as large dust storms and volcanic eruptions. Aerosols are highly mobile; they can cross oceans and mountain ranges. It is generally agreed that skies in many parts of the world are hazier than they were one or two centuries ago, even in rural areas.

The major parts of aerosols consist of water soluble substances, and act as condensa tion nuclei for drop formation if they possess the appropriate size. This so called nucleation scavenging means that the aerosols and their attached radon progeny

are rinsed to the ground during rain fall. The precipitation can also hit aerosols, both water soluble and non soluble, not yet in a rain drop, and consequently drag it along on its way to the ground (impact scavenging or sub cloud scavenging). During snow fall the counter part is called snow scavenging. The fraction of progenies not attached to aerosols and the fraction of radon dissolved in water should also be rinsed out and dragged to the ground through these scavenging processes. In addition to this physical rinsing process the radon left in the air has a lower probability of interaction with aerosols after disintegration, as the total aerosol concentration is lower (ERNBO, 2006).

Not only does the amount of rain fall affect the aerosol concentration. It is also strongly affected by conditions such as humidity and pollution (including dust and smoke) which in turn depend on wind direction. Humidity increases aerosol coalescence, and is a function of temperature why this is another important factor. The transportation of aerosols, as well as atmospheric matter, including the Radon gas itself, is dependent on the general state of the atmosphere. It is subjected to stratum, temperature deviations, different wind speeds and wind directions. Stable strata result in a low vertical mixing, while turbulence and instable strata yield increasing mixing processes (ERNBO, 2006).

The fate of newly generated radon daughters in air can be very complicated. But the basic processes in defining *unattached* and *aerosol attached* products are two steps. The first step is the reaction, in less than one second, of newly born ^{218}Po radionuclide with trace gases and air vapors. The result of this reaction is particles of diameter ranging from 0.5 to 5nm known as clusters or unattached radionuclides. Freshly formed atoms of ^{218}Po are mostly (95%) positively charged and hence quite mobile. These properties makes them react with trace gases and vapors in air very fast so as to form small clusters or unattached rdionuclides with diameter ranging from 0.5 to 5 nm. In a normal mine, this unattached fraction of ^{218}Po is nearly 0.05.

The second process involves the attachment of the cluster radionuclides to already existing aerosol particles, in the atmosphere with in 1 to 100 seconds, to form radioactive aerosols. Therefore decay of radon gives rise to daughter products which occur in the forms of free ions, atoms or in the form of radioactive aerosols.

1.3 Aerosols and Radon Decay in the Atmosphere

More than 90% of the Radon daughters are positively charged. The free ions with a positive charge tend to attract water molecules present in air in order to form what is commonly known as cluster (CLR) (Hawarynski & Domanski, 1982). This

cluster formation is attributed to the attraction between the charged daughter and the high dipole moment (6.2×10^{-30}cm) of water molecules. In addition to reaction with vapors the ions may also react chemically with oxygen and trace gases such as SO_2, SO_3. Most of these small particles will grow to aerosol attached daughters in air. However, a fraction of the daughter product concentration in air remain free (unattached) radionuclides in air.

The parameters influencing the proportion of attached and unattached radionuclides are the; Diffusion Plateout; Deposition; aerosol concentration.

1.3.1 Diffusion of clusters

The mobility is characterized by the diffusion coefficient that chiefly controls the formation of the radioactive aerosol by attachment and the deposition on surfaces in human lung. Studies concerning the diffusion coefficient of ions in air goes back to the second decade of this century. Some results, for the case of the first daughter product of radon (^{218}Po), based on experiments and computations based on theoretical models are cited in table 1.2.

Table 1.2: Measured /Computed values of diffusion coefficients of Rn Diffusion Coefficient (cm^2/s)

	Diffusion Coefficent (cm2/s)	Remark
Chamberlain and Dyson (1956)	0.054	
Madelaine (1966)	0.005 – 0.06	
Raabe(1968)	0.047 –0.035	Relative humidity 15% - 35%
Thomas (1970)	0.085	For atoms of average age less than 15 to 20 sec and Rel humidity>20%
	0.053	Under very dry conditions
Kotrappa and Mayya (1976)	0.005 0.095	For RaC For RaA
Porstendorfer and Mercer(1978)	0.024	Relative humidity < 2%
	0.068	Relative humidity >30%
Hawrynski and Domanski(1982)	0.0202 – 0.0091	Relative humidity 5% -10% Computed based on theoretical model.
Wellish (1994)	0.045	

With the exception of the measurements by Porstendörfer and Mercer (Porstendörfer & Mercer, 1978), all measurements show decrease in the diffusion coefficient with increase in humidity. This agrees with the experiments carried out by McLaughlin as described below.

1.3.2 Aerosol Concentration

The fraction of the activities of RaA and the other daughters in the attached state increases as the aerosol concentration is increased. The fraction of the total RaA atoms in the attached state, for an unventilated room under equilibrium conditions given by (Stranden & Berteig, 1982):

$$1 - f = \frac{bz}{\lambda_1 + \lambda_d^a} \frac{\lambda_1}{\lambda_1 + \lambda_z + \lambda_d^f}$$

Where
z=the aerosol particle concentration
b = attachment coefficient
λ_1 = deposition or plateout rates. Superscripts f and a represent deposition rate for the free and attached radionuclides respectively.
λ_1 = $3.78 \times 10^{-3} \mathrm{s}^{-1}$ is decay constant.
f = the attached fraction.

The attached plateout rate is always less than the plateout rate of the unattached. From the above equation it is seen that the bz term is dominant at high concentration. Using typical values b= 10^{-6}cm^3/sec; f = 2E^{-3} sec^{-1} and a=5E^{-5} sec^{-1},for room condition, it follows that

1-f =0.14 when z=103/cm^3 1-f =0.98 when z=106/cm^3

1.3.3 Attachement Rate

Wicke and Prostendoefer have shown that the attachment rate R of radon daughter atoms to atmospheric aerosol is a linear function of the concentration (Z) of the aerosol particles.

R = β Z

Where β is mean attachment coefficient. It is also shown that is constant when the aerosol concentration is raise from 0.5E^4/cm^3 to 10E^4/cm^3. The dominant of the parameters influencing the values of f and 1-f, as discussed above is thus the aerosol concentration in air.

Despite all the works on the attached and unattached fractions in the past two decades, researchers are reflecting their reservation regarding the practical importance of the classification it self. Busigin etal were the first to conclude that the diffusion coefficient of "unattached" ^{218}Po in air could not be adequately described by a single number, given the experimentally observed range of 0.005–0.1 cm^{2}s^{-1}. Measurements of diffusion coefficient of ^{218}Po shows its diffusion coefficient is a function of the length flow rate ratio of the diffusion tube. This fact alone leads to the conclusion

that there exists no unique diffusion coefficient. Based on this observation Busigin etal (1981) hypothesized for the first time that the diffusivity depends upon the chemical nature of the reaction product formed between ^{218}Po and the gaseous environment.

The apparent discrepancy between the measured diffusion coefficient of ^{218}Po and what is expected from kinetic theory, is one evidence for the so called unattached ^{218}Po atoms are not a single species.

Joshi and Kekar (1982) suggested that the observed size distribution of radon daughters (median size and geometric standard deviation) is a more useful parameter in calculating their health effects than classifying them as attached and unattached fractions.

Measurements of lung deposition of radon daughters, shows that it is necessary to determine the entire size distribution of the radioactive aerosol, for proper calculation of lung dose. In filter method of sampling radon in air, the availability of nearly 100% efficient filters made it unnecessary to make correction for unattached fraction while measuring air sampled on a filter.

Early studies established two different types of aerosols of radon progeny attached and unattached. Aerosol behavior of most of the progeny is similar to that of ordinary ambient aerosol particles in the atmosphere. Therefore, because radon progeny atoms are created one at a time from the parent Rn gas, scientists have assumed that these radon progeny atoms are attached to the already present atmos pheric aerosol particles. This assumption is supported by measurements of the particle size distributions of Rn progeny (Johnson et al., 1991).

When radon atom decays through the emission of an alpha particle, the positively charged heavy metal decay product quickly forms a small cluster with other molecules in the air. Such clusters are called unattached radon progeny (ERNBO, 2006). This unattached fraction, more highly diffusive species, (figure 1.3 a and b) (Po, Pb, Bi) rapidly combine with other aerosols in the atmosphere (e. g . H_20 , $S0_2$, NO_x) to form particles whose sizes are in the range of 0.5 to 5 nm. These particles form what is known as the attached fraction. The size and the magnitude of the unattached fraction is important because Rn progeny that reach the trachea, and are in the unattached size range, have a much higher probability of depositing on the surfaces of the bronchial airways than do particles whose sizes are more characteristic of ambient aerosols (50-500 nm). The unattached fraction of Rn progeny can therefore significantly and disproportionately affect the radiation doses to the conducting airways of the lung (Johnson et al., 1991).

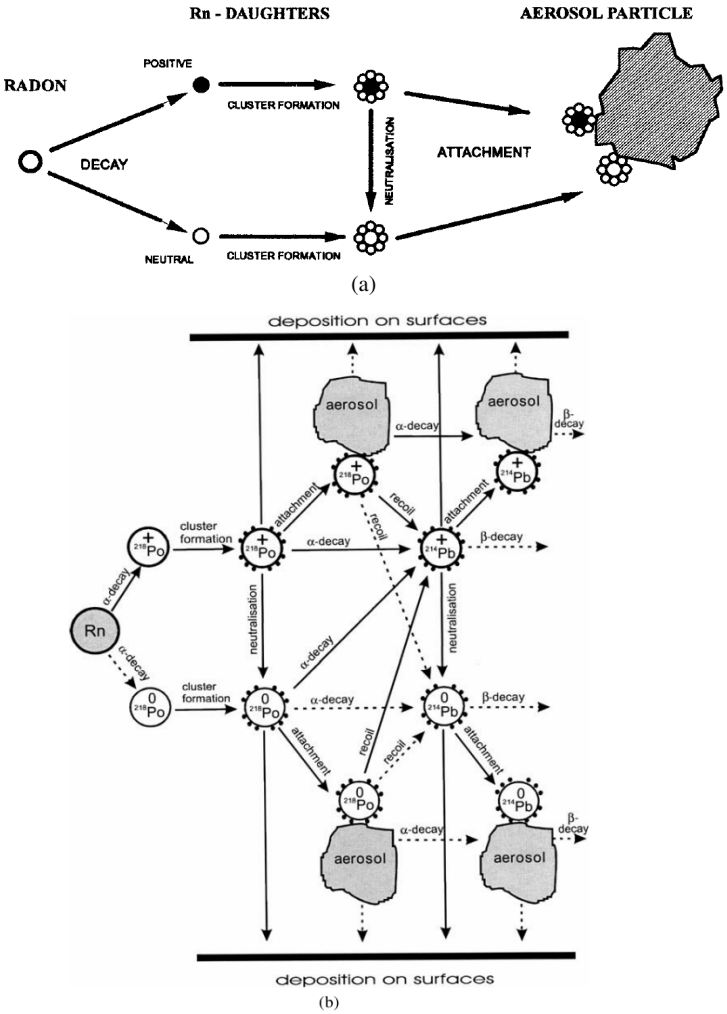

Figure 1.3: (a) Basic processes of radon decay product behaviour in air defining *unattached* and *aerosol-attached* particle activities. (b) Processes of ^{218}Po and ^{214}Pb in air (Papastefanou, 2008).

1.4 Deposition of Aerosols in the Respiratory Tract

Deposition of inhaled aerosols is one of the most important issues in the human respiratory tract models. The deposition model is needed to provide the fraction of inhaled aerosols to be deposited in the human lung. The ICRP66 deposition model estimates the total deposition fraction (if the quantity of aerosol particles deposited in the entire respiratory tract is divided by that inhaled, the result is called total deposition fraction or total deposition) and the regional deposition, i.e. deposition in each anatomical region of the respiratory tract. The new ICRP 66 HRTM is represented by five regions(fig 1.4): Extrathoracic (ET), thoracic bronchial (BB), bronchiolar (bb) and alveolar interstitial (AI), based principally on radiobiological

considerations, but also taking in to account differences in function, deposition and clearance. Deposition in ET region is determined empirically by a new ICRP 66 HRTM. For thoracic airways, a theoretical model of gas transport and particle deposition is used to calculate the deposition in each of BB, bb and AI regions to quantify the effects of subject′s lung size and breathing rate. The regional fractional deposition is calculated for aerosols having log normalized particle size distributions with geometric standard deviations taken to be a function of median particle size.

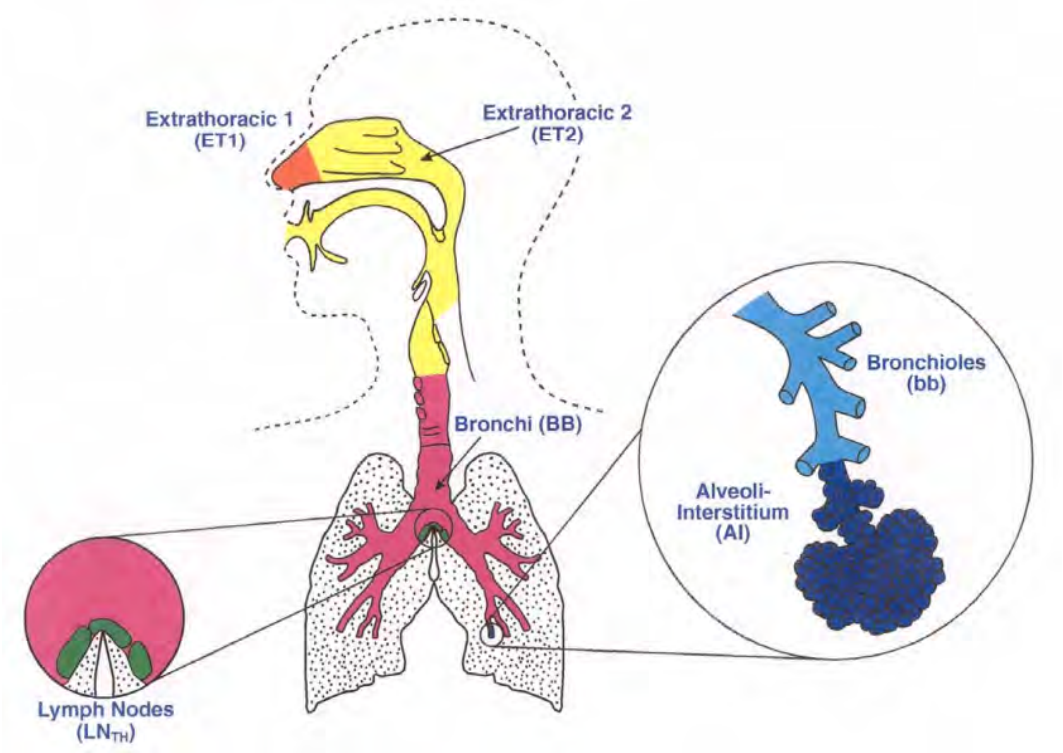

Figure 1.4: anatomical compartments ICRP 66 lung model (Boecker, 1995)

It has been known for many years that exposure to an atmosphere containing radon can increase the risk of lung cancer. It is now understood that the most important component of the dose comes not from the gas itself, but rather from its short lived decay products. Radon itself is an inert gas with a half life of 3.8 days and almost all the gas that is inhaled will be breathed out again (Kendall & Smith, 2002). When Radon (neutral) transfer to Radon progeny after emit alpha (charged) and beta (charged) particles the decay product or radon progeny will be formed the progeny are being chemical active and solid element isotopes. They will quickly attract themselves to molecules of water and other atmospheric gases or attach to natural aerosol particles. This aerosols are mixed in air and they enter into the human lung during inhalation. If inhaled, the decay products, whether attached to aerosol particles or unattached, will largely be deposited on the surface of the respiratory tract and, because of their short half lives (less than half an hour) will

decay there. A fraction of them is deposited in the lung, depending on the size, density, shape, charge, and surface properties of the particles of the aerosols and the breathing pattern of the individual, while the rest is ejected from the body during exhalation (Heyder, 2004), (Yu et al., 2006).

Aerosols deposited when inhaled air with aerosol passes through respiratory tract; when inhaled air passes through nasopharnex or oralpharynx then trachea which divides into the right and left bronchi and separate into secondary lobar branches and sub segmental branches, then dividing into smaller quaternary branches numb ering more than 800. This branching extends into smaller conducting airways and level of the terminal bronchioles. After terminal bronchioles separate into respiratory bronchioles that nearly 150,000. Then in to respiratory bronchioles divide into alveolar ducts that are almost entirely lined with alveoli; there are about 26 million of these ducts giving rise to 50 to 100 million alveolar sacs, here gas exchanged due to movement of diaphragm pressure because of alveolar walls are composed of reticular and elastic fibers then these air back to all steps which it pass during inhalation then fraction of aerosols deposited equal amount of efficiency during inhaled and exhaled in each regions.

In the course of normal respiration, rates of air flow entering the respiratory tract may range from zero to a maximum of 1000 to 2000 ml/s, depending up on the amount of work being performed. During both inspiration and expiration, deposition processes that follow physical laws will take place. The three principal mechanisms of deposition are inertial impaction, sedimentation, and diffusion. Particle deposition as a function of electrical charge (image diffusion) is believed to be of secondary importance except where very highly charged particles are generated. Deposition mechanisms are greatly influenced by changes in air flow and by the differences in residence times at each level of the respiratory tract that occur during each cycle of complete respiration. At a ventilation rate of 200 ml/s, linear air flow rates will range from 180 cm/sec in the main bronchi to only 0.025 cm/sec in alveolar ducts (Stuart, 1984).

1.5 Mechanisms of Deposition

The deposition of an inhaled aerosol occurs through three mechanisms as shown figure 1.5. The first is inertial impaction, in which a droplet fails to turn a corner and impacts the wall of the airway. The second is sedimentation, in which the droplets or particles *rain out* under the influence of gravity. Finally, there is diffusion caused by Brownian motion, which results in eventual collisions of the droplets with the airway wall (Allan L. Coates, 2008). Generally we classified them two groups of deposition processes, i.e Thermodynamic and Aerodynamic deposition.

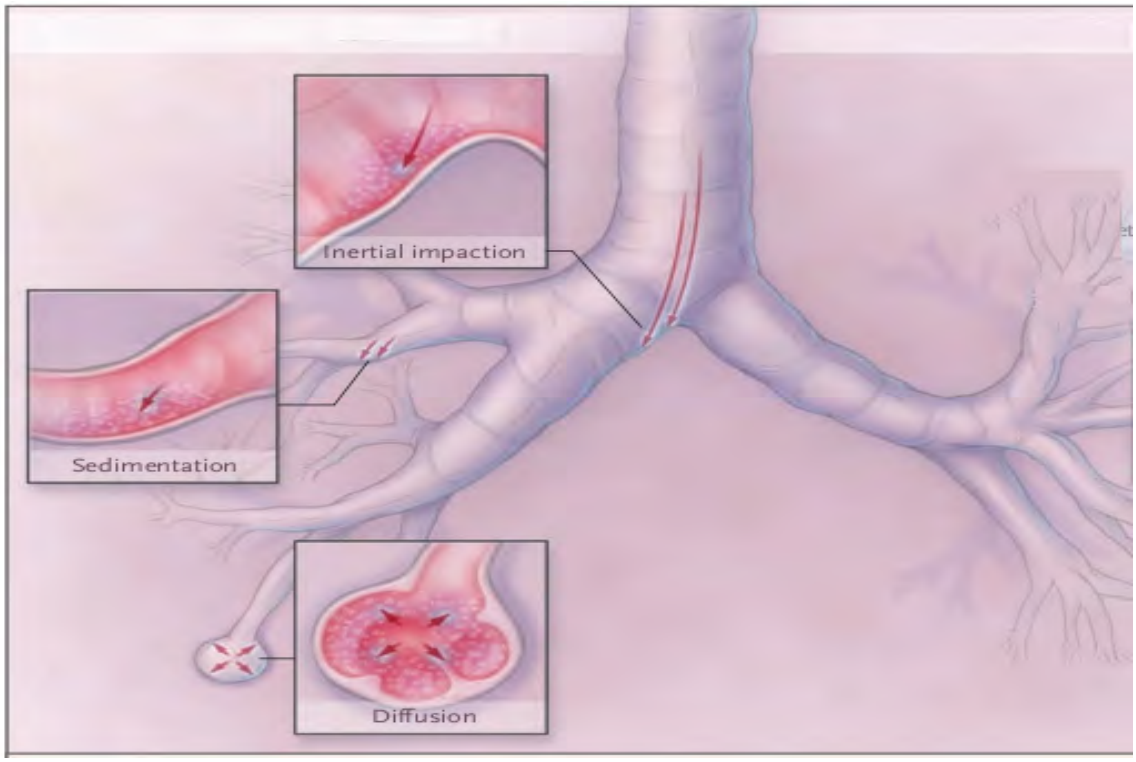

Figure 1.5: There are three conventional modes of particle deposition in the lung: inertial impaction, sedimentation, and diffusion. Red arrows show the movement of particles (Allan L. Coates, 2008).

1.5.1 Thermodynamic Deposition

Thermodynamic deposition is important for particles less in size or the particle smaller than 1 μm in diameter are slowly deposited due to diffusion they often called diffusion or Brownian deposition. These particles are displaced by the random thermal motion of the gas molecules of air. This displacement Λ is inversely proport ional to the viscosity of the air γ and to the diameter of the particle d_{ae}, and it is directly proportional to the residence time t of the particle in a given air space:

$$\Lambda = [(RT/N)(Ct/3\Pi\gamma d_{ae})]^{1/2} \tag{1.7}$$

where R, T and N are the ideal gas constant, the absolute temperature, and Avogad ro's number, respectively and C is Cunningham's correction. Thus the probability of deposition by diffusion D will increase as the displacement motion is increased relative to the size of the confining space :

$$D = 1 - exp(-0.58\Lambda/R) \tag{1.8}$$

This type of deposition is caused by the random movement of the aerosols in the air stream. When the aerosols *touch* the wall of the airway tube, they can stay in that position. The distance of a particle travels by diffusional transport increases with decreasing particle size and increasing respiratory cycle period (decreasing

respiratory rate) and as a result there occurs a minimum deposition at which the displacement velocity due to terminal settling is low and the displacement velocity due to diffusion is also low (Stuart, 1984). Total diffusional deposition there fore decreases with increasing particle size up to about 1 μm becomes negligible for larger particles and predominates for very small particle sizes (Heyder, 2004), (Yu et al., 2006).

1.5.2 Aerodynamic Deposition

Aerodynamic deposition is more important for larger particles and there are two types of processes belonging to this group. The first one is *impaction* or inertial deposition. This is the principal mechanism of large particle deposition in the upper regions of the respiratory tract, acting on particles ranging from 2 to 3 μm to greater than 20 μm in gases diameter. This deposition process takes place when the air stream changes the direction; some of the airborne aerosols with larger mass cannot adjust their directions of movement sufficiently quickly because of their inertia, and impact onto the wall of the airway tube. The probability I of inertial deposition is proportional to the terminal settling velocity V_t of the entrained particle, times the velocity of the air stream V_a and inversely proportional to the radius R of the airway (Stuart, 1984):

$$I \propto (V_t V_a \sin\theta)/gR \tag{1.9}$$

where g is the gravitational constant. The larger particle, the greater settling velocity. At increasing air velocity, greater bend angles θ and smaller airway radii, there will be greater probability of deposition by inertial impaction (Heyder, 2004), (Yu et al., 2006).

The second aerodynamic deposition process is gravitational sedimentation of aeroso ls. In sedimentation, the particles suspended in air slowly *rain out* under the force of gravity. Because the smaller particles have a greater ratio of surface area to weight than larger particles, they remain suspended longer and may be exhaled before deposition (Allan L. Coates, 2008).

Sedimentation, or settling under the force of gravity, is an important deposition mechanism for particle in the respiratory tract. Gravitational sedimentation becau se of it gravity dependent so that alveoli at the base of the lung are relatively compressed compared alveoli are more compliant ventilation is greatest near to the bottom of the lung and became progressively reduced near the top (Chantal Darquenne & Prisk, 1997).

Sedimentation, or settling under the force of gravity dependency as follow; a particle falling in air accelerates to a terminal settling velocity V_t at which the force of

gravity is balanced by the resistance of the air (Stuart, 1984):

$$V_t = (\rho - \sigma) g d_{ae}^2 / 18\gamma \tag{1.10}$$

where γ is the viscosity of air, and ρ and σ are the densities of the particle and of air, respectively. As the particle diameter d_{ae} becomes very small, i.e., of the same order as the mean free path of air molecules (A), air resistance decreases, and a correction factor must be applied (Stuart, 1984):

$$V_t(actual) = V_t(calculated)[1 + (2A\lambda/d_{ae})] \tag{1.11}$$

where A = 1.26 + $0.4^{-(1.1 d_{ae}/2X)}$. This terminal settlin velocity may be approximated as $2.9 \times 10^5 \times (\rho d_{ae}^2)$ cm/sec.

As shown in fig.1.6, generally we can say that total diffusional deposition decreases with increasing particle size up to about 1 μm and becomes negligible for larger particles, in the size range of 0.1 up to 1 μm, particles are simultaneously deposited by gravitation and diffusion. For larger particles, thus, in the size range above 1μm particles are deposited due to impaction and sedimentation increase with increase size.

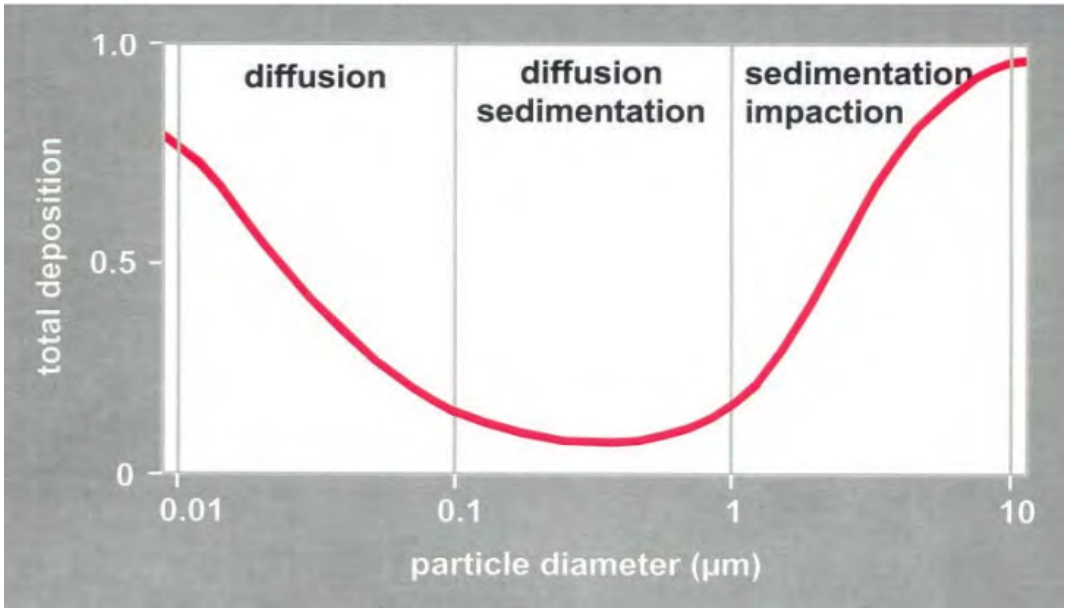

Figure 1.6: Total deposition of unit density spheres in the human respiratory tract inhaled orally at rest.

Deposition occurs in all compartments of the human lung, but with different efficien cies. The deposition pattern depends on the aerosol diameter as well as airflow characteristics.

The behavior of small size particles (which are deposited by diffusion) is described in terms of the thermodynamic diameter d_{th} and the diffusion coefficient D. Deposition of larger particles is described by the aerodynamic diameter d_{ae}. The aerodynamic

diameter is defined in terms of the equivalent particle volume diameter d_e (i.e., the diameter of a spherical particle with the same volume as the considered particle) by the following formula (Yu et al., 2006):

$$d_{ae} = d_e \sqrt{\frac{\rho C(d_e)}{X \rho_o C(d_{ae})}} \tag{1.12}$$

where ρ is the particle density, ρ_o = 1 g cm^3 (unit density), X the particle shape factor (its value is usually between 1 and 2), and C is the so called Cunningham′s correction slip factor given as:

$$C(d_e) = 1 + \frac{\lambda}{d_e}[1.514 + 0.8exp(-0.55(d_e/\lambda))] \tag{1.13}$$

where λ = 0.0712 μm is the mean free path of air molecules at 37 ^{o}C , 100% relative humidity and 760 mmHg atmospheric pressure. The parameter d_{ae} appears on both sides of Eq. (1.13) and iterations should be used in order to determine d_{ae} . The thermodynamic diameter is given in terms of its aerodynamic diameter by the following equation:

$$d_{th} = d_e \sqrt{\frac{X \rho_o C(d_{ae})}{\rho C(d_{th})}} \tag{1.14}$$

This equation, again, needs to be solved by iterations in order to find d_{th} (Yu et al., 2006).

CHAPTER 2
REVIEW OF RELATED LITERATURE

2.1 DISCOVERY AND RISKS OF RADON

2.1.1 Discovery of Radon

In 1899 Ernest Rutherford and R. B. Owens founded that the radio activity of thorium compound could be below away. They were studding the emanations from thorium and wrote that the radiation from thorium was not constant but varied in a sudden unexpected changes. Rutherford made a key observations such that, the emanation act likes ordinary gas and that the intensity of radiation fallen to one half of its value after an interval of about one minute (Bemenet Alemayehu, 2006).

In 1900, Frederick Dorn a German scientist found that ^{226}Ra was giving off a gas which he called *radium emanation* known today as ^{222}Rn. Dorn and Rutherford confirmed that the emanation from radium were a radioactive gas. And in 1991, it was perfectly shown by the discoverers that the emanation stayed for 7.64 days besides to its being gas. Marie and Pierre Curies were the first to observe that the emanation from Radium is radioactive. It was not known, to the Curies, the gaseous state of the emanation which was the back bone of the discovery. Ramsay and Gray in 1908 isolated enough of the gas to study its physical properties and named it Niton (the shining one). In 1904, Mache introduced the first unit for radon activity concentration and called it Mache Enheit that was replaced in 1910 with the Curie. Mache used a galvanometer similar to the one used by Curie to measure the ionization current. One Mache (ME), corresponds to 13.5 Bq/L (364 pCi/L) and 37 Bq/m^3 or (1pCi/L) = 0.0028 ME.

Another naturally occurring isotopes of radon were also discovered by Rutherford and Owns, ^{220}Rn (Thoron), half life 55.5s in 1899. Friedreich Giessel and Andre Lousi Debjerne also showed the existence of an other isotope called actinon (^{219}Rn) half life 3.8s in 1904. It is known that there are around 36 isotopes of radon in addition to the above two. Some of these isotopes are man made while others are naturally occurring with less than five percent natural abundance (Tsega Berhane Teklu, 2007). In 1901, Rutherford and Brooks demonstrated that Rn is a radioactive

gas. Rutherford, in the same year discovered the active deposits of thorium and the Curies discovered the active deposits of radium. In 1902, Rutheford and Soddy characterized alpha particles when they worked on thorium compounds (George, 2008). The first radon measurement made by Elster and Geitel in 1901 was basically intended for the study of environmental phenomena like atmospheric electricity, atmospheric transport and exhalation of gases from soil. Serious investigations were followed not for atmospheric studies but to a great extent due to the health hazards caused by radon. Series of measurements world wide have shown that radon is the ubiquitous part of the atmospheric air.

2.1.2 Discovery of Risks of Radon

Although, radon was discovered in 1900, the effects of prolonged exposure had been noted about 300 years earlier. Georgius Agricola, a German physician and geologist landmark publication De Re Metallica (On the Subject of Metals), in 1556. This information was published in his book (1494-1555), noted a high frequency of fatal lung diseases occurring among local miners: In 1527 he was a key figure in helping to advance numerous safety factors in mines, some useful and some not so useful (Lewis, 2006). Georgius introduced various forms of mine ventilation, masks worn over the mouth and face. Paracelsus a Swiss physician and scientist (1493-1541), studied the diseases of underground miners in the Erz Mountains of Eastern Europe and found that many miners died from lung disease, concluding that dust and gases present in the mines were the cause of it. Agricolo was Italan physician, in 1533, in his book, he indicate his familiarity with the occupational diseases and hazards of mining. He described the effects of cold and wet conditions, heavy metal toxicity and accidents. He also recorded the respiratory diseases of miners, and attributed them to dust that penetrates into the windpipe and lungs (Craven & Smit, 2006).

As early as the sixteenth century a high incidence of lung disease was recognized among certain underground miners in eastern Europe. In 1879, two physicians Harting and Hesse, found that the mortality rate of uranium miners who worked in Germany and Czechoslovakia to be near 75 %. The German miners who worked more than 10 years developed the Erz Mountain disease which was later identified as lung cancer. In 1921, Margaret Uhlig, was the first to suggest that the radium emanation might well be the cause of lung cancer. Three years later in 1924, Ludewig and Lorenser suggested that the lung cancers of these miners might be caused by the radon gas in the mines. During 1924-1932, the finding of high concentrations of radon in the region and in the near by mines of Joachimstal in Chechoslovakia and in Radium mines of Schneeberg Germany, suggested that radon was the cause of the high lung cancer incidence. In 1932, Pirchan and Sikl,

concluded that the Radium emanation causes lung tumors among the miners at Jachymov. Over half the deaths were from lung cancer and most occurred among miners before they reached the age of 50 (George, 2008).

The hypothesis that radon decay products caused lung cancer was not accepted by some, until the findings of epidemiological studies of underground miners in the 1950s and 1960s. The findings of the BEIR Report VI, which was based on underground mine data and laboratory studies showed that from 60,000 miners who worked between 1941-1990, in different groups of mines in 8 countries, over 2,600 developed lung cancer where only 750 were expected. From 20 epidemiological studies of underground miners, eleven studies provided quantitative information on the exposure response relationship between radon and lung cancer risk. In the past 5 years, the epidemiological study in Iowa US in particular, showed a high incidence of lung cancer among women exposed to high radon levels in residential buildings. As a result of these studies, both in the underground mines and in residential studies support very strongly the characterization of radon concentration levels and the assessment of the radiation dose from radon found in different environments (George, 2008).

The causative relationship between high radon concentration in mine air and excess incidence of lung cancer in miners was not determined through epidemiological research until fairly recently. Even more recently, many underground miners have been studied with respect to exposure to Rn progeny and the observed incidence of lung cancer. These populations have included both uranium miners and other hard rock miners. As a result, it is now generally accepted that inhalation of Rn progeny has led to increased incidences of lung cancer in underground miner populations, and that the magnitude of the increased cancer incidence is related to the cumulative exposure, and therefore the cumulative radiation dose, to the miner (Johnson et al., 1991).

More recently, Saccomanno in 1996 found that smokers who are also miners have a 9.3 % higher incidence of lung cancers than non mining smokers and that lung cancer was increased in cigarette smoking miners and non miners, but that the proportion of lung cancers in the *central zone* was significantly greater in miners than in non miners. Craven & Smit (2006), conclude that inhaled dust, Radon and cigarette smoke combine to form large particles that deposit in the central bronchial tree, but that filtered smoke free of dust form smaller particles that deposit more peripherally. Obviously, the non miners were exposed to only home or free air Radon levels, and the distribution of the cancers in miners and non miners clearly differed (Craven & Smit, 2006).

It is clear, from the multiplicity of factors that play a role in determining the biological effects of inhaled radioactive materials, that no simple relation between

gross atmospheric concentration of a radioisotope and lung effects can be assumed. Conservative criteria, derived from physiologically based biokinetic models of the human respiratory tract (HRT), are therefore used when setting safety standards for airborne radioactivity. Radiation dosimetry and calculation of inhalation and acceptable atmospheric concentrations of radioactivity are based on dosimetric models of the respiratory tract. The first such dosimetric model was introduced by the ICRP (Cember & Johnson, 2009).

2.2 HUMAN RESPIRATORY TRACT MODELS

2.2.1 Theoretical Model

Work Related to Lung Model

Dosimetric modeling of the respiratory tract started soon after Second World War in 1949 in relation to the enhanced necessity for nuclear technology and uranium ore exploring. The needs for standardization of values for parameters describing inhalation, deposition, retention and translocation of air borne radionuclide in workers for the purpose of deriving exposure limits were recognized. The first ICRP conference devoted to dosimetric models of the human respiratory tract was held in 1949 at Chalk River, Canada. Different aspects of aerosol particle deposition and retention were discussed, and the large deficiency of information was noted. It was agreed that 50% of any inhaled aerosols reached the alveoli and that soluble particles would be completely absorbed. If the aerosol particles were insoluble, half of them would be retained for 24 h, and half of the remaining (25% of inhaled quantity) would be retained in definitely. In the following meetings, different parameters which could influence the deposition and retention of inhaled aerosols were identified. These parameters included the particle size and shape, surface area available for deposition, and breathing habits (nose or mouth breathing), etc.

This very simple model of the deposition was slightly improved in 1953 at the Arden House Conference when it was assumed that 50% of inhaled aerosols were deposited in the upper part of the respiratory tract, 25% would be exhaled and 25% would be retained in the lungs. If the particles were soluble, 25% would be absorbed and translocated to different organs in the body. For insoluble particles, 12.5% would be cleared in 24 h, and the remaining 12.5% would be retained with a half time of 120 d. This model of deposition, retention and clearance of inhaled aerosol particles was the basis for the limits for exposure to radionuclide in ICRP Publication 2 as well as for the calculation of doses to exposed individuals (Yu et al., 2006).

In 1964, the ICRP Committee 2 appointed a Task Group on Lung Dynamics to review the previous model published in the ICRP Publication 2. Two years later, In 1966, a new lung model was published with a greatly improved lung deposition and clearance models. The ICRP Task Group on Lung Dynamics, TGLD, published a comprehensive report on models of the deposition and retention of inhaled particles in the human respiratory tract. This information was the basis of the dosimetric model for the respiratory tract included in the recommendations of the ICRP in its Publication 30.

In the 1979 model, the respiratory tract was divided into the three airway regions, (nosopharyngeal, tracheo bronchial tree and pulmonary), and the term *anatomical compartments* were introduced. The deposition models in different compartments were based on dust sampling data. This 1966 model also considered particle size and breathing rate with respect to the fraction deposited in different region of the lungs. The second important feature was the quantitative kinetic clearance model that described the removal of materials deposited in each of the three regions. The new concept was the classification of chemical compounds according to their tendency to be dissolved in the respiratory tract fluids, which was known as the DWY classification. Class D referred to highly soluble compounds that were cleared from the respiratory tract with clearance half time less than 1 d. Class W referred to less soluble compounds that were cleared from the respiratory tract with clearance half time of a few days to months. Finally, Class Y referred to more insoluble compounds that were expected to be retained in the respiratory tract with half time of 6 months to 1 year (Yu et al., 2006),(Boecker, 1995).

Publication 30 model most of the absorbed radiation dose to lung is received in the P region because of the longer retentions that occur in this region. Except for clearance from compartment f with a half time of 1 d, clearance from compartments e, g, and h all occur with the half times associated with the classification of the inhaled material, i e., 0.5, 50, or 500 d for Classes D, W, or Y, respectively. In this model, the long term clearance of radionuclides from the P region by either mechanical transport or dissolution absorption processes is described by the Same half time, a simplification that makes the model difficult to apply to particles in which the dissolution absorption and mechanical clearance processes lead to substantially different half times. A related aspect of this issue is the extent to which one or more of these processes differs from the other in a time dependent way. The 1979 model does not account for such differences. Thus, the classification of inhaled particles as Class D, W, or Y involves a number of assumptions and compromises that make the model difficult to use in many analyses of site or process specific exposure scenarios.

However, this greatly improved model was not formally accepted for dose limit

calculations until 1979 when the new ICRP 30 Publication was prepared. In this publication, the derived air concentration and the annual limits on intake were introduced. Furthermore, the transfer of radioactive materials to the lymph nodes was included in this model. These models calculated the dose for many organs and tissues so that control could be based on weighted doses to a number of organs and tissues instead of just a critical organ. Organ retention patterns were defined better by using sums of exponential functions to describe both short and long term retention components, Models for various elements had differing degrees of biological significance. But in the total mass of the blood filling lungs, and they did not recognize specific sensitive cells in the epithelium. Filtration in nasal passage was also not considered in this model (Yu et al., 2006),(Boecker, 1995)

Since 1966, many extensive investigations in the field had been undertaken, and many deficiencies of the model were observed. The most important criticism was addressed to the DWY classification of chemical compounds. Many materials were cleared from the human respiratory tract at rates considerably different from the predicted ones. On the other hand, some materials did not fit any of the categories in the classification. A very important case was found for inhalation of the highly insoluble plutonium oxide which was cleared with a rate smaller than that for the Y class (Yu et al., 2006).

In addition, investigations had extended to particles with diameters smaller than those considered in the 1966 model. The model presented in the ICRP 30 is related to the occupational exposure of reference Caucasian males. However, in the last two decades, interest had been raised about public exposure to radioactivity in the environment. A new model was therefore necessary to enable dose calculations for other members of the population as well as for other ethnical groups in the world. Radiobiological investigations had shown large differences in radio sensitivity of different cells in the respiratory tract. In ICRP 32, the dose was calculated in basal cells in the bronchial epithelium and in the pulmonary region. Half of the stochastic risk was associated with these regions, which was contradictory to the previous concept of mean lung dose used in ICRP 30. Further radiobiological studies had included secretory cells as target cells at risk.

All these new findings and deficiencies of old models had requested for a new respiratory tract model. As a result, the ICRP formed a new Task Group on Lung Dynamics in 1984 in order to review the old model and to propose modifications and improvements of the existing respiratory tract model. The new model appeared in 1994 (the ICRP66 model) in ICRPP publication 66 (Yu et al., 2006).

ICRPP publication 66 is the newest model, the 1994 , is divided into five airway regions. The extrathoracic airway divided into two compartments: ET1, the anterior nose, and ET2, the posterior nasal passages, larynx, pharynx, and mouth. The

bronchial region, BB, consists of the trachea and bronchi (16 bronchial airway generations), starting with the trachea as generation 0 and ending with the terminal bronchioles as generation 15. In this model, the bronchial (BB) region comprises generations 0 to 8, while the bronchiolar (bb) region ranges from generation 9 to 15. And the bronchiolar region, bb, consists of the bronchioles and terminal bronchioles. The last region, the alveolar interstitial region, AI, consists of the respiratory bronchioles, the alveolar ducts, alveoli, and the interstitial connective tissues (Boecker, 1995),(Hofmann, 1998).

This new dosimetric model is the result of increased knowledge of the biokinetics of the respiratory processes involved in the inhalation of aerosols and gases, the radiosensitivity of the several different tissues within the respiratory tract, and the biological effects of inhaled radioactivity. This increased knowledge makes the new model applicable to all population groups, old and young, male and female, and at different levels of physical activity (heavy exercise, light exercise, resting, and sleeping), rather than only to occupationally exposed, unisexual adults at work. It accounts for the effects of other air pollutants and for smoking, and considers respiratory disease and the health status of the individual (Cember & Johnson, 2009).

Softwares that implemented the ICRP66 model were available, namely, the LUDEP program and its smaller version RADEP for radon. In addition to these, there were several home written programs that follow ICRP66 recommendations. These softwares enabled calculations of DCCs and analyses of influence different relevant parameters on the lung dose.(Yu et al., 2006)

Deposition Efficiency

There are several studies were have been conducted to measure the deposition in humans respiratory tract using of monodispersed insoluble aerosols, assessed as a function of different parameters.

The first comprehensive theoretical treatment of total respiratory tract deposition was developed by Findeisen in 1935, based on a model consisting of the trachea, four generations of bronchi, two generations of bronchioles, alveolar ducts and alveolar sacs; the results are shown in Figure 2.1. Landahl in 1950 described a model including mouth and pharynx with two orders of alveolar ducts; using 3/8 of the respiratory cycle for inspiration and 3/8 for expiration (curves 2,3,4 of Fig. 2.1). In 1949 Sinclair and LaMer developed a generator that produced mono dispersed aerosols, i.e., aerosols of a single particle size. These were used in tests by Landahl in which fractions of exhaled air were collected and analyzed. Altschuler examined deposition of mono dispersed aerosols of density 1.3 g/cm^3, finding a deposition minimum at 0.4 μm, as predicted by their model, and that

slow, deep breathing increased deposition. In 1965 Beeckman examined Landahl′s model using computer simulations to determine the effect of recycled non deposited aerosols and interpulmonary gas mixing (curve 5); this model predicted decreased total deposition as tidal volume was decreased. Dennis used stearic acid particles to study total respiratory tract deposition; fractions increased as respiration rates were lowered below 15 cycles/min (curve 10). Curve 11 presents studies of coal dust deposition made by Walkenhorst and Dautrebande Davies derived formulas based on continuity between suspended and deposited aerosol fractions for prediction of deposition fractions (Stuart, 1984).

In 1959 the International Commission on Radiological Protection (ICRP) developed a working model to describe roughly the deposition of inhaled dust. They assumed 75% of the mass of all inhaled dust was deposited, with 25% exhaled. Two thirds was deposited in the upper respiratory tract (i.e., from the exterior nares to the larynx), and one third in the lower respiratory tract, with differing clearance patterns, for soluble or insoluble dusts. This extremely simple model provided the initial design of safety procedures involving airborne radioactive particles, but ignored the effects of particle size and density on deposition fractions, and did not describe deposition sites that could be correlated with subsequent clearance patterns (Stuart, 1984).

The Task Group on Lung Dynamics was established in 1966 by the International Committee on Radiological Protection to develop a deposition model for inhaled particles using data based on a three compartment model of the respiratory tract. The nasopharynx consisted of the anterior and posteriornares, plus the oralpharynx; the tracheobronchial region extended from the larynx to the terminal bronchioles, composed of airways having ciliated epithelium; the pulmonary region included respiratory bronchioles, alveolar ducts, alveolar sacs and alveoli; i.e., the gas exchange region of the lung. It was based on the real world conditions that air contaminants are usually inhaled as dispersed aerosols that can be frequently described by log normal distributions of particle diameters. Deposition fractions were described in terms of the aerosol particle size distribution, i.e., the mass median aerodynamic diameter (MMAD). Values for deposition by diffusion were obtained by the use of the Gormley Kennedy equations for laminar flow in tubes. Reasonable agreement was obtained between predictive deposition curves for monodispersed particles and the experimental results of Van Wyck and Patterson, as wel as Dautrebande and Walkenhorst and Dennis. Little variation was found for aerosols of widely different degrees of dispersity of particle sizes within an aerosol; i.e., different geometric standard deviations. Similar curves were found for tidal volumes of 750, 1450 and 2150 mL, suggesting that although an individual′s minute volume (tidal volume times respiration rate) controls the total amount of dust inhaled and deposited, it

has relatively little affect on deposition fractions (Stuart, 1984).

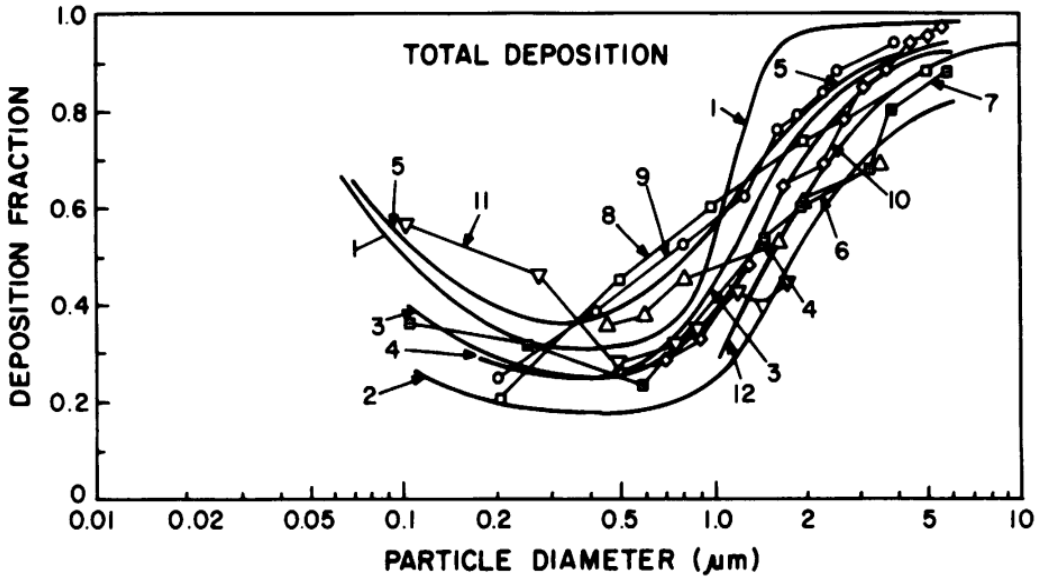

Figure 2.1: Predictive models and experimental values for total deposition of inhaled particles: (1) predictive, Findeisen, 200 mL/sec, 14 respirations/min; (2) predictive, Landahl, 300 mL/sec, 5 respirations/min, tidal volume 450 mL; (3) predictive, Landahl, 300 mL/sec, 7.5 respirations/min, tidal volume 9000 mL; (5) theoretical, Beeckmans , 5 respirations/min, tidal volume 1350 mL; (6) experimental, Wilson and LaMer, 5.5 respirations/min; (7) experimental, Landahl , 7.5 respirations/min, tidal volume 900 mL; (8) experimental,Gessner, 15 respirations/min, tidal volume 700 mL; (9) experimental,Van Wijk and Patterson, 19 respirations/ min, tidal volume 700 mL; (10) experimental, Dennis, 13.3 respirations/min, tidal volume 720 mL; (11) experimental, Dautrebande and Walkenhorst, 10 respirations/min, tidal volume 990 mL; (12) experimental, Davies, 15 respirations/ min, tidal volume 600 mL(Stuart, 1984)

Pattle in 1961 studied nasal deposition of monodispered methylene blue particles produced by a spinning disk generator. The fractional nasal penetration of inhaled particles was expressed by the empirical relationship:

$$P = 0.95[1 - 51\log(d_{ae}^2 Q/20.2)] \tag{2.1}$$

Here d_{ae} is the particle diameter (μm) and Q is the flow rate in liters/minute. Nasal deposition N for particles of aerodynamic diameter (d_{ae}) was expressed as:

$$N = -0.62 + 0.475\log(d_{ae}^2 Q) \tag{2.2}$$

This equation was used by the TGLD to determine deposition in the nasopharyngeal region. Particles of the largest inhalable size ($< 100\mu$m) down to about 20μm were calculated to deposit quantitatively in the nasopharyngeal region. In 1971 Hounam developed equations for nasal deposition of inhaled insoluble particles and measured deposition in the nasopharynx N of pressure differential P_{nm}, between nose and mouth (Stuart, 1984);

$$N = -0.975 + 0.66 \log(d_{ae}^2 P_{nm}) \tag{2.3}$$

Data obtained from human volunteers were the basis for estimates of regional deposition in the thoracic region. The Task Group on Lung Dynamics (1966) adopted an empirical relationship for nasal deposition of particles based on in vivo data of Pattle (1961) for particles $> 1\mu$m in diameter. The deposition efficiency was expressed as a function of the inertial parameter ($d_{ae}Q$), where d_{ae} is the aerodynamic diameter, and Q (L min^{-1}) (Cheng, 2003).

$$\eta_N = -0.62 + 0.475 \log(d_{ae}^2 Q) \tag{2.4}$$

This inertial parameter (d_{ae}^2Q) becomes the Stokes number ($\frac{d_{ae}^2 Q/9}{\mu LA}$) if a characteristic length (L) and cross sectional area (A) of the nasal airway geometry are used, where μ is air viscosity. (1981) derived similar deposition equations in nasal and oral airways by summarizing in vivo deposition data from several studies with two logarithmic functions of the inertial parameter. Their analysis showed great variability of deposition efficiency in both nasal and oral regions under similar experimental conditions. These equations have been used in many lung deposition models to predict regional dosimetry of inhaled particles. However, these analyses are limited. Because of the variability of the data sets, it is not possible to confirm the assumption that the head airway deposition is a unique function of the inertial parameter. The fitted equations predicted over 100% deposition at larger values of the inertial parameter, indicating that the equation may not show the correct mathematical form of the deposition mechanism. The aerosol deposition should range from 0 to 1. At small values of the inertial parameter, the deposition approaches zero, indicating no deposition due to inertial mechanism; on the other hand, at large values of the inertial parameter, the deposition efficiency should approach 1 (Cheng, 2003).

The NCRP/ITRI deposition model is based on the model of Yeh and Schum (1980) divided respiratory tract into three main regions: the naso oro-phar-yngolaryngeal (NOPL), tracheobronchial (TB), and pulmonary (PI regions. The major modifications to the Yeh and Schum model (1980) are briefly described as follows:

1. **Nasal and oral deposition:** Data for ultra fine particles became available during the last ten years. Because the structures in the nasopharyngeal

region are extremely complex, empirical equations are often used to calculate nasopharyn geal deposition. For particle diameters $> 0.2\mu$m , measurements of nasal and oral deposition have been reported. These data, summarized by K.N. Yu 1981, were fit by log logistic functions and can be written as:

$$N_i = 1/[1 + (\rho d_{ae}^2 Q/4600)^{-0.94}] \tag{2.5}$$

$$N_e = 1/[1 + (\rho d_{ae}^2 Q/2300)^{-1.01}] \tag{2.6}$$

$$O_i = 1/[1 + (\rho d_{ae}^2 Q/30000)^{-1.37}] \tag{2.7}$$

$$O_e = 0 \tag{2.8}$$

(assumed if no other information),(Yeh et al., 1996) where N_i , and N_e, are the nasal deposition efficiencies during inspiration and expiration, respectively; O_i and N_i, are the oral deposition efficiencies during inspiration and expiration, respectively; ρ is the particle density (g/cm^3); d_{ae} is the particle diameter (μm); and Q is the average flow rate (cm^3/sec). For particle diameters $< 0.2\mu$m, data from Cheng were used. These can be written as:

$$Ni = 1 - exp(-12.8Q^{-1/8}D^{1/2}) \tag{2.9}$$

$$Ne = 1 - exp(-15.0Q^{-1/8}D^{1/2}) \tag{2.10}$$

$$Oi = 1 - exp(-57.1Q^{-1/8}D^{2/3}) \tag{2.11}$$

$$Oe = 1 - exp(-48.8Q^{-1/8}D^{2/3}) \tag{2.12}$$

where D is the diffusion coefficient (cm^2/s) of the particles. Inhalability: Before particles can deposit in the respiratory tract, they must be inhaled from the ambient air. It follows that particles that do not enter the nose or mouth are unavailable for deposition.

2. Inhalability is defined as the fraction of the suspended material in ambient air that actually enters the nose or mouth with the volume of air inhaled. For the NCRP/ITRI model, the inhalable fractions defined by the American Conference of Governmental Industrial Hygienists were adopted:

$$E = 50(1 + exp(-0.06d_{ae})) \quad \text{for } 0 < d_{ae} \leq 100\mu\text{m} \tag{2.13}$$

where E is the fraction of ambient air borne particles that are inhalable and d_{ae}, is the particle aerodynamic diameter.

3. **Correction for diffusional deposition in the TB region:** Because of the nature of the airway branching in the TB region, the air flow enters a daughter airway segment from the parent airway segment (or vice versa)

at an angle (branching angle). The effect of this entrance configuration is the enhancement of diffusional deposition. In their experimental study of ultrafine particle deposition in a human tracheobronchial cast, Cohen in (1990) reported that the measured deposition is about twice thapredicted based on the Ingham equation for a straight tube. Because this effect can be attributed to the presence of turbulence, secondary flow, developing flow, and the branching angle at the entrance of the daughter airway segment in the branching airways suggested the following equations to correct for the entrance configuration effect:

$$P_D^E = 1 - (1 - P_D)^{f_e} \tag{2.14}$$

$$f_e = 1 + C_1(2R/L), \quad \text{for } L/R > 10 \tag{2.15}$$

(2.16)

P_D given	$\theta = 90^o$ P_D^E	P_D^E/P_D	$\theta = 45^o$ P_D^E	P_D^E/P_D	$\theta = 20^o$ P_D^E	P_D^E/P_D
0.00001	0.000024	2.40	0.00002	2.00	0.0000152	1.52
0.0001	0.00024	2.40	0.0002	2.00	0.000152	1.52
0.001	0.0024	2.40	0.002	2.00	0.00152	1.52
0.01	0.0238	2.38	0.0199	1.99	0.0152	1.51
0.05	0.116	2.32	0.0975	1.95	0.0749	1.50
0.1	0.223	2.23	0.19	1.90	0.148	1.48

Table 2.1: Calculated Ratio of P_D^E/P_D (Yeh et al., 1996)

where P_D^E = diffusion deposition probability, taking into account the effect of the entrance configuration; P_D = predicted diffusion deposition; $C_1 = (2\theta/\Pi)(13 - 12\theta/\Pi)$; and θ = bend angle or branching angle (in radians). The empirical enhancement based on their study on the effect of entrance configuration factor in equation (2.15) was given by on heat transfer coefficients in circular tubes. Equation (2.14) was derived based on heat and mass transfer analogy. Table1 2.1 hows the ratio of P_D^E/P_D, for θ = 20^o, 45^o, and 90^o. P_D, usually is < 0.1 for any airway segment, and θ ranges from 18^o to 51^o. This ratio of P_D^E/P_D ranging from 0.48 to 2.4 is compatible with the values reported by B. S., Sussman, R. G., and Lippmann in 1990.

4. **Use of the model for infants and children:** The Yeh and Schum model was adapted for use in infants and children by scaling the airway dimensions and using an appropriate ventilation rate according to R. F., Cuddihy in 1985.

5. **Application to polydisperse aerosols:** In the home or workplace, the aerosols are usually polydisperse. To predict the initial regional respiratory tract

deposition pattern after polydisperse aerosols are inhaled, the program was modified to integrate the deposition over the size distribution. The user needs only to specify the aerosol size distribution (e.g., mass median diameter and geometric standard deviation) in addition to the other usual parameters (such as breathing frequency, tidal volume, functional residual capacity, pause between breaths, etc.) (Yeh et al., 1996).

In the new lung deposition model of the International Commission on Radiological Protection (ICRP) (ICRP 1994), nasal and oral deposition equations were obtained using a different mathematical form:

$$\eta = 1 - \frac{1}{(ad_{ae}^2 Q + 1)} \tag{2.17}$$

The Task Group of the National Council on Radiation Protection and Measurement (NCRP) in 1996; and NCRP 1997 used a slightly different deposition equation:

$$\eta = \frac{1}{1 + (\frac{\rho d_{ae}^2 Q}{a})^{-b}} \tag{2.18}$$

Using these equations, the deposition efficiency η approaches 1 for large values of the inertial parameter and 0 for small values of the inertial parameter. Later, experimental deposition in physical casts of extrathoracic airways showed that for ultrafine particles $\leq 0.2\mu$m, deposition increases with decreasing particle size and flow rates, indicating diffusion deposition for ultrafine particles. Based on a turbulent diffusion model, deposition efficiency can be expressed as a function of diffusion coefficient (D) and flow rate Q:

$$\eta = 1 - exp(-aD^{0.5}Q^{-0.125}) \tag{2.19}$$

Values of constant a were estimated from fitting the curves of experimental data for nasal and oral deposition. This equation wasused in the new ICRP (1994) and NCRP (1996) lung deposition models. In vivo deposition data of head airways for ultrafine particles and radon progeny confirmed the data from physical casts. In vivo data also show intersubjectvariability in the diffusion deposition regime (Cheng, 2003).

In the past decade, studies with physical casts and computational fluid dynamic simulation have improved the understanding of deposition mechanisms. Extrathoracic airway dimensions were also measured in detail. Nasal airway geometry showed great variability among groups of adult volunteers. Furthermore, diffusion deposition of the nasal airway has been associated with airway geometry (Cheng, 2003).

In 1999 Sarangapani and Wexler together study the influence of dispersion on particle deposition in the lung. They show that dispersion influences on the total

deposition of inhaled particles and in particular increases the pulmonary deposition of fine mode particles. They also discuss how dispersion can help elucidate a number of clinical and epidemiologic results associated with particle deposition in the lung (Sarangapani & Wexler, 2000).

2.2.2 Experimental Model

To simulate particle deposition, the respiratory tract is modeled as a pre-filter followed by a successive series of filters. The pre-filter represent the nares and the anterior nasal airways. Each of the successive filters represents the successive anatomical regions in the respiratory tract. Therefore, smaller fractions of the inhaled particles pass through each successive filters. In this model, filtration occurs during both inhalation and exhalation. Using this model, and considering the simultaneous deposition mechanisms of inertial impaction, gravitational settling, and diffusion of particles in the respiratory tract, deposition fractions for each region (Cember & Johnson, 2009).

Cheng and Yeh (1980) developed and verified a theoretical equation from fan model filtration theory to describe particle penetration through a wire screen. The theory has permitted the calculation of the particle size versus penetrability characteristics of the various stages of a graded screen array system depending on the screen parameters and sampling face velocity (Hayes, 1991).

The deposition of particle in nasal cavity and in the tracheobronchial region of respiratory tract by using multiple metal wire screens to mimic the deposition properties of Rn progeny in the nasal (N) and tracheobronchial (T-B) regions, was designed by Hopke, Ramamurthi and Knutson in 1990. Based on the modified version (Ramamurthi and Hopke, 1989) and Yeh and Schum (1980); the deposition relations given by Yu and Diu (1982) for laminar flow diffusional deposition, deposition by impaction and sedimentation; the correction factors given by Cohen, Sussman and Lippman (1990) for incomplete development of uniform laminar flow. Again, they were successful in using four layers of 400-mesh wire screens with a face velocity of 12 cms^{-1} for the simulation of Rn progeny deposition in the T-B region. The formula derived from the experimental data of the penetration of ultrafine particles through a nasal cast experimental wire screen collection which done by Cheng and yeh (Hopke et al., 1990), (Yu et al., 2001). In similar way,in 2004, bronchial deposition was calculated by T. T. K. Cheung and K. N. Yu, to get bronchial dosimeter from radon progeny, for home exposure. This model consists of five 400-mesh wire screens with a sampling face velocity of 3.3 cms^{-1} and 2.7 cms^{-1} for Chinese males and females respectively. The deposition pattern on the wire screens were found to satisfactorily match the variation of the dose conversion coefficients with the size of radon progeny from 1 to 1000 nm. The bronchial dosimeter for mine

exposures consists of four 250-mesh wire screens with a sampling face velocity of 3.3 cms^{-1}. The deposition pattern on the wire screens were found to satisfactorily match the variation of the dose conversion coefficients for both Chinese males and females (Cheung & Yu, 2004).

Based on the work of Hopke, simple method used by A. C. George and E. O. Kuntuson to measure this deposition. The sampler was designed to simulate the particle collection properties of the nasal and tracheobronchial parts of the respiratory tract. In their work a change in the original design on the nasal deposition. The original design consists of the sampling filter and screen filter heads to be operated simultaneously. One head collects the total aerosol on filter. The second contents a single 100-mush stainless steel wire screen that simulates the collection characters of the human nose. The third head contains a single 100-mush wire screens which together simulate the combined collection characteristics of the nasal and the nasal plus tracheobronchial regions, respectively. The sampling flow rate is 157 cm^3s^{-1} for each head resulting in the a face velocity of 12.0 cms^{-1} on the screen.

The system defers from design specification given by Hopke in thata 100 mesh screen was used in but in their in place of single 400 mesh screen to reproduce the collection characteristics of the nasal cavity. This change was made to reflect new experimental evidence and changing opinions about the deposition particle in the nose. At the time Hopke′s article was written, it was believed that nasal deposition for any particle size could be calculated from the empirical equation of Cheng. Further experiments using unattached ^{222}Rn or ^{220}Rn progeny have shown that the earlier equation over predicted deposition for 1nm particles and this has lead to a new fundamentally deferent equation. In the old equation the collection efficiency in the nose dependent exponentially coefficient whereas the new equation employs the 1/2 power. The 100 mesh screen was chosen because it fits the new equation better than the 400 mesh particularly in the vicinity 1nm (George & Knutson, 1992).

The effect of gravity on deposition of 0.5 to 3μm diameter aerosol in the human lung, done by Darquenne, Chantal, Manuel Paiva, John B. West and G. Kim Prisk (in 1997). Intrapulmonary deposition of 0.5, 1, 2, and 3μm diameter particles in four subjects on the ground (1 G) and during parabolic flights both in micro gravity (μG) and at 1.6 G were measured. Subjects breathed aerosols at a constant flow rate (0.4 l/s) and tidal volume (0.75 liter). At 1 G and for 1.6 G, deposition increased with increasing particle size. In μG, differences in deposition as a function of particle size were almost abolished. Deposition was a nearly linear function of the G level for 2 and 3 μm diameter particles, whereas for 0.5 and 1 μm diameter particles, deposition increased less between μ G and 1 G than between 1 G and 1.6 G. Comparison with numerical predictions showed good agreement for 1, 2, and 3

μm diameter particles at 1 and 1.6 G, whereas the model consistently underestimated deposition in μG. The higher deposition observed in μG compared with model predictions might be explained by a larger deposition by diffusion because of a higher alveolar concentration of aerosol in μG and to the non reversibility of the flow, causing additional mixing of aerosols (Chantal Darquenne & Prisk, 1997).

CHAPTER 3
METHODS

3.1 CHENG'S METHOD

Cheng (2003) studied and analyzed data to obtain deposition equations in the extrathoracic region for nasal and oral breathing, respectively. In several studies, the nasal airway dimensions for casts and human volunteers have also been measured. Under the assumption that the airway geometry is a major factor in deposition, it was then possible to include the relevant airway dimensions in the deposition equation to explain the inter subject variability of deposition in the in vivo experiments. The inertial mechanism for particles > 0.5 μm and the diffusion mechanism for particles < 0.5 μm dominate deposition in the nasal and oral airways. A turbulent deposition flow in the extrathoracic air ways was assumed, so the deposition equation could be expressed as

$$E = 1 - exp(-aStk - bSc^{-1/2}Re^{-1/8}) \tag{3.1}$$

where Stk (d_a^2 U/9μL), Sc (ν/D), and Re (UL/ν) are the Stokes, Schmidt, and Reynolds numbers, respectively. The first term of the argument is for the impaction mechanism, and the second is for the diffusion mechanism. For particles $>1\mu$m in size, the diffusion term is negligible compared to the inertial term, and the deposition efficiency can be approximated as

$$E = 1 - exp(-aStk) \tag{3.2}$$

On the other hand, for particle sizes < 0.1 μm, the diffusion term is dominant, and it can be simplified as

$$E = 1 - exp(-bSc^{-1/2}Re^{-1/8}) \tag{3.3}$$

As the Stokes number increases, Eq.(3.1) and (3.2) approach 1, whereas for ultrafine particles Eq. (3.1) and (3.3) approach 1 as the value of $Sc^{-1/2}$ $Re^{-1/8}$ becomes large. The minimum deposition occurs for particle sizes between 0.1 and 1 μm when both inertial and diffusion effects are at a minimum.

Cheng using data were obtained using two nasal airway replicas made from MRI scans with detailed airway dimensions, which constructed using a series of 3 mm coronal magnetic resonance imaging (MRI) scans of the nasal airways. The replicas

were composed of 3 mm thick clear plastic layers. Constant inspiratory flow rates of 7-50 L min^{-1} and 5-20 L min^{-1} were used for the deposition study. Assuming that the critical dimension is the minimum cross sectional area in the nasal passage, a dimensionless Stokes number can be calculated (Stk = $\Pi^{0.5}$ d_a^2 Q/18$\mu A^{1.5}$) as a function of the aerodynamic diameter (d_a), flow rate (Q), and the minimum cross-sectional area (A_{min}). A_{min} of the adult obtained by MRI scans are 1.61 cm^2 , and he arrive deposition efficiency expressed as

$$E_n = 1 - exp(-110Stk) \tag{3.4}$$

He suggests that impaction deposition is the dominant deposition mechanism in the nasal airway passage for particles > 1.0 μm.

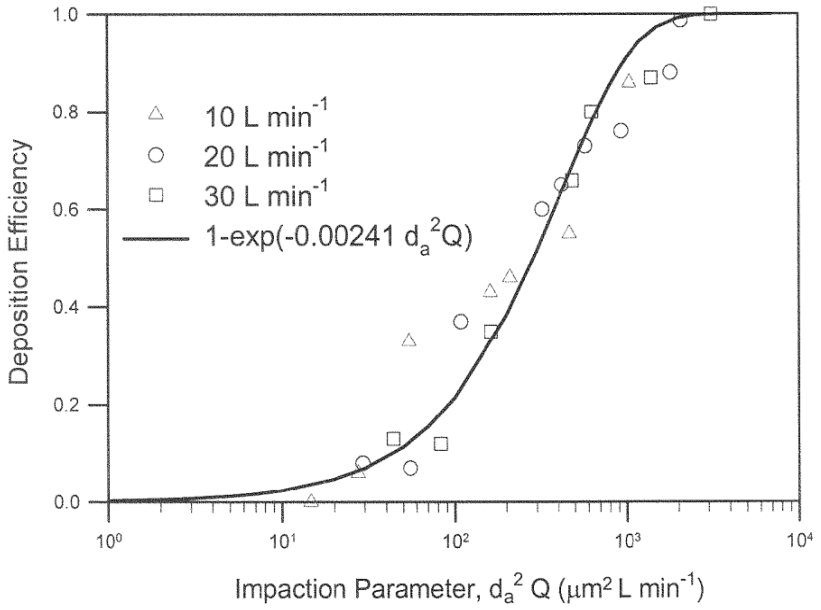

Figure 3.1: Nasal deposition efficiency excremental and curve-fit (Swift 1991).

3.2 SERIAL BOLUS DELIVERY METHOD

Theoretical Analysis

When a mono disperse aerosol is inhaled with a tidal volume of V_T, deposition fraction (DF) of the aerosol in the lung can be obtained by measuring the number of aerosol particles inhaled N_{in} and exhaled N_{ex} breath by breath as follows

$$DF = 1 - N_{ex}/N_{in} \tag{3.5}$$

Here, the aerosol fills the entire volume of V_T, and deposition takes place throughout the lung regions where V_T communicates. DF in this case is also defined as total lung deposition fraction (TDF). This traditional aerosol inhalation mode may be divided into a series of aerosol bolus inhalations: The volume V_T is divided into a

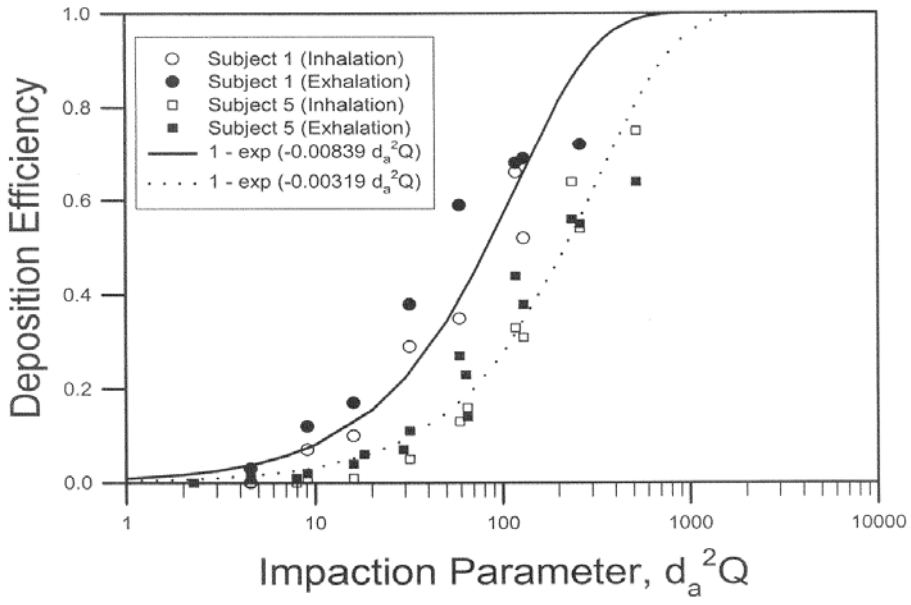

Figure 3.2: Nasal deposition efficiency excremental and curve-fit for adult and child airway replicas (Swift 1991).

number of smaller compartments with equal volume, and a series of inhalations is performed with the same V_T in which the aerosol fills only one volumetric compartment in each inhalation, as shown in Fig.3.3. TDF will then be obtained by

$$TDF = \frac{1}{n}\sum_{i=1}^{n}(1 - RC_i) \tag{3.6}$$

where n is the total number of volumetric compartments and RC_i $(= N_{ex}/N_{in})$ is the recovery of bolus aerosol from the i^{th} compartment.

If particle deposition efficiency in the i^{th} compartment is defined by X_i and deposition efficiencies are the same on inspiration and expiration, the deposition amount in each volumetric region as a fraction of inhaled bolus can be calculated as illustrated in Fig. 3.3, where i^{th} is defined by the amount of aerosol depositing in a volumetric compartment i divided by the amount entering the compartment. In Fig. 3.3, expressions for inspiratory and expiratory deposition are shown on the top and bottom of each volumetric compartment, respectively. The fraction of aerosol that is available for exhalation at end inspiration is shown on the right hand side of each bolus inhalation diagram. Recovery of bolus aerosol from the i^{th} compartment is then expressed by

$$RC_i = \prod_{k=1}^{i}(1 - X_k)^2 \tag{3.7}$$

Values of i^{th} can then be obtained from the ratio of RC values from two adjacent compartments as

$$RC_i/RC_{i-1} = (1 - X_j)^2 \tag{3.8}$$

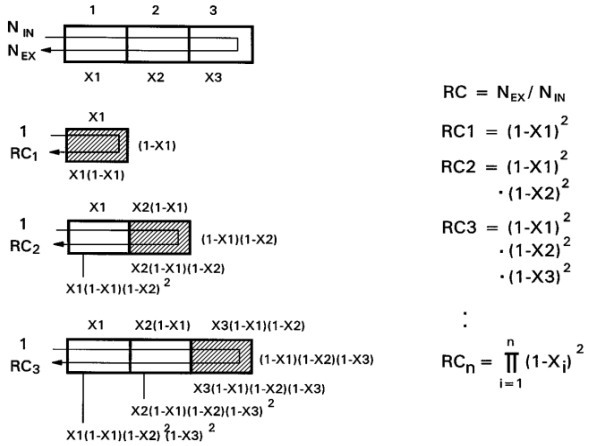

Figure 3.3: Calculation procedures for deposition efficiency (X_i) and deposition fraction in local lung regions in a serial compartment lung model. Top: 3 compartment model ($i = 1-3$). Aerosol recovery (RC_i) and bolus deposition fraction in each compartment (BDF_{ij}) are shown for each sequential bolus inhalation ($j = 1 - 3$). Values of X_i were assumed to be the same on inspiration and expiration. Expressions for inspiratory and expiratory BDF are shown on top and bottom of each compartment, respectively. Aerosol fractions remaining at end inspiration are shown on right of each diagram. Right: expressions for RC. Expressions for RC and BDF are shown as a fraction of inhaled aerosol.N_{in} and N_{ex}, number of inhaled and exhaled particles.

$$X_j = (1 - RC_i/RC_{i-1})^{\frac{1}{2}} \tag{3.9}$$

Once i^{th} values have been obtained, the deposition fraction of a bolus aerosol in each volumetric compartment (BDF$_{ij}$) can be obtained by combining the inspiratory and expiratory deposition in each compartment shown in Fig. 3.3. The subscript j represents the number of sequential bolus inhalations. The local deposition fraction (LDF) in the i^{th} compartment (LDF$_i$) and TDF of non bolus VT aerosol can then be obtained by

$$LDF = \frac{1}{n}\sum_{j=1}^{n} BDF_{ij} \tag{3.10}$$

and

$$TDF = \sum_{i=1}^{n} LDF_{ij} \tag{3.11}$$

where n is the total number of volumetric compartments of V$_T$ or the number of sequential bolus inhalations. Therefore, total as well as regional lung deposition can be determined by measuring the recovery of aerosols from a series of bolus inhalations.

subject No	Age (yr)	Height (cm)	Fvc (ml)	FEV_1 (ml)	FEV_1/FVC	TGV (ml)	Raw (cm) $H_2O.1^{-1}$ (s)
1	21	181	5,303	4,148	0.78	2,849	1.59
2	22	184	5,021	4,636	0.92	3,389	0.56
3	22	189	5,221	4,922	0.94	3,420	0.47
4	30	175	4,923	4,164	0.85	3,028	1.25
5	22	179	5,374	4,618	0.86	2,666	1.00
6	25	184	7,650	6,170	0.81	4,484	1.04
7	32	173	4,959	3,783	0.76	2,324	2.74
8	28	191	5,089	4,283	0.84	3,350	1.02
9	28	176	4,759	4,044	0.85	3,402	0.71
10	22	177	5,678	4,487	0.79	3,773	1.19
11	27	182	5,638	4,071	0.72	4,475	1.05
Mean ±SD	25 ± 4	181 ± 5	5,419± 757	4,484± 617	0.83 ± 0.06	3,378 ± 647	1.15± 0.59

Table 3.1: Subject characteristics and lung function test results

Experimental

Subjects: Healthy nonsmoking men (n = 11) were recruited locally (age 19 -38 yr). The subjects had no history of smoking within 1 yr and no history of hay fever or asthma. All subjects underwent a screening procedure that included a complete medical history, physical examination, SMA 20 blood chemistry screen, and complete blood count with differential. For those who passed the initial screening, their basic lung functions were measured by spirometry and body plethysmography. All subjects were asked to read and sign a consent form approved by the Institutional Review Board of the University of North Carolina School of Medicine. Subject characteristics and lung function test results are given in Table 3.3.

Generation of test aerosols

Monodisperse di-2-ethylhexyl sebacate (DES) oil aerosols were generated by an evaporation condensation type aerosol generator (MAGE, Lavoro E Ambiante, Bologna, Italy). The performance characteristics of the MAGE generator have been described previously. In the present study the original MAGE generator was modified to improve the quality of aerosols and to generate large size particles. Briefly, aqueous solutions of NaCl (5 - 10 mg/l) were nebulized by a Collision type atomizer that was operated with compressed nitrogen gas (20 psi). Liquid aerosols generated initially were passed through a drying column filled with silica gel, and the resulting dry nuclei aerosols (1 - 3 l/min) were passed through a boiler in which DES oil was heated and vaporized at 170 - 250 ^{o}C . The mixture of nu.clei and DES oil vapor from the boiler was passed through a reheater that was maintained at 280 - 320 ^{o}C and subsequently through a vertical condensation column that was designed to induce condensation of vapor on the surface of nuclei particles. Mono disperse DES aerosols emerging from the condensation column were diluted with clean air (20 - 100 l/min) by use of a two stage diluter. By changing the concentration of

nuclei and the temperatures of the boiler and the reheater, we generated mono disperse aerosols with 1, 3, and 5-μm diameter (geometric SD $<$ 1.15) particles. Particle size was measured by an aerodynamic particle sizer (model 33B, TSI, St. Paul, MN) equipped with an on line aerosol diluter (1:100 ratio; model 3302, TSI). Concentration of aerosols was maintained at a level of 2 $\times$ 10^3 - 40 $\times$ 10^3 particles/cm^3 depending on particle size: Higher concentrations for smaller particle size and vice versa.

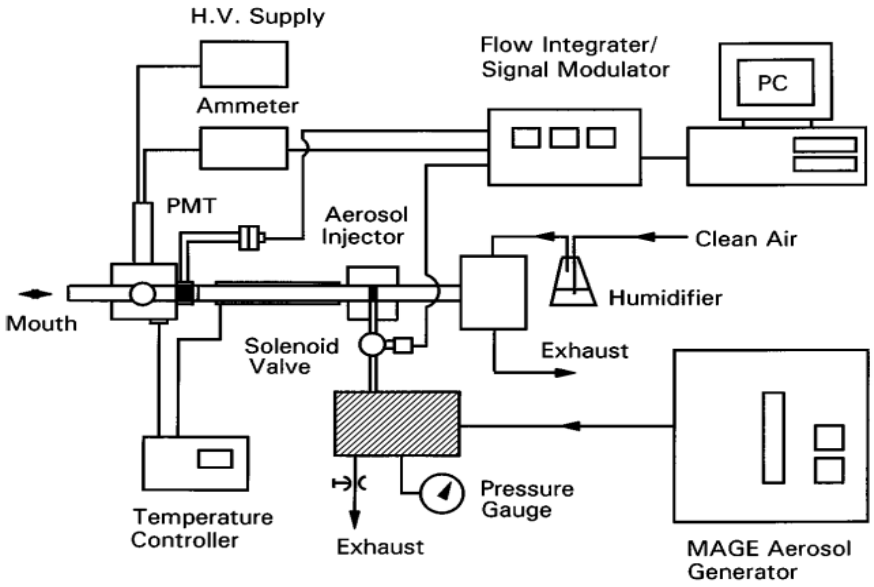

Figure 3.4: Experimental system used for aerosol bolus inhalation. PMT, photomultiplier tube; HV, high- voltage.

Bolus aerosol inhalation system

The core of the system consisted of a laser aerosol photometer, an aerosol bolus injection module, and an on line data acquisition system (Fig 3.4). Test aerosols were introduced into the aerosol photometer as a small pulse (half width = 45 ml) by activation of a solenoid valve in the bolus injection module. When the valve was open, an aerosol was ejected into the inspiratory air stream via four narrow slits (1.6 mm wide, 18 mm long) positioned across the diameter of the stream. The aerosol chamber upstream of the solenoid valve was maintained at slightly above room pressure (1 - 5 cmH_2O) to help inject the aerosol. The multiple slit system was designed to ensure a rapid mixing of aerosol with the inspiratory airflow, thereby producing a well-defined small bolus. In the laser photometer, a laser beam (15 mW He-Ne, Melles Griot, Carlsbad, CA) was expanded into a thin sheet via a cylindrical lens and shone through an aerosol detection cell where the laser beam was scattered by aerosol particles. The scattered light was collected on a photomultiplier tube (model 9798B, EMI Gencom, Plainview, NY), and the signals from the photomultiplier tube were amplified to 0 - 10 V with a current amplifier

(model 427, Keithly Instruments, Cleveland, OH) and subsequently transmitted to the data acquisition system. The aerosol detection cell was heated to 40 ^{o}C by an electric resistor embedded in the metallic block of the cell to prevent moisture condensation on the lens during exhalation. Flow rates through the laser photometer were measured by a pneumotachograph (Fleisch no. 1) in conjunction with a pressure transducer (model 239, 61.27 cmH_2O range, Setra Systems, Acton, MA) connected directly to the inspiratory inlet of the detector cell. The data acquisition system consisted of a signal modulator and a personal computer (model 326, Dell Computer, Austin, TX) equipped with a high-speed data acquisition board capable of sampling signals at up to 27 kHz (model DT 2801A, Data Translation, Marlboro, MA). Flow and aerosol signals were displayed digitally in the signal modulator in which a built-in integrator circuit provides volume signals for inhaled and exhaled air. The volume signals were used to activate the solenoid valve and to deliver an aerosol bolus to a prescribed lung depth. For on line data acquisition, flow and aerosol signals were acquired at a rate of 200 Hz, and flow signals were smoothed by passing them through a 50 Hz low pass filter to eliminate spikes generated by the activation of the solenoid valve. Smoothing of aerosol signals was not necessary. All the controls for bolus inhalation, data acquisition, and analysis were programmed with ASYST software (ASYST Software Technologies, Rochester, NY).

Inhalation procedure

After a few practice breaths, the subject inhaled filtered air via a laser aerosol photometer (25 ml dead space volume) from functional residual capacity (FRC) following a prescribed breathing pattern displayed on the computer screen. The subject then activated the data acquisition mode by pressing a hand-held switch during expiration, inhaled a prescribed volume, and exhaled to residual volume (RV) at a constant flow rate (Fig. 3.5). During the data acquisition mode, a small aerosol bolus (,45 ml half width) was introduced into the inspiratory stream by opening an aerosol valve for a predetermined duration of time. The duration of valve opening was adjusted between 50 and 250 ms, depending on flow rate, to maintain a consistent bolus volume: the faster the flow rate, the shorter the duration. The peak concentration of bolus was maintained at 6 - 9 V; 1 V was equivalent to ,5,000 particles/cm^3 for 1μm diameter particles. The bolus was delivered to a lung depth (V_p) of 100 - 500 ml in 50 ml increments. This procedure was repeated with mono disperse aerosols of three different particle sizes [1, 3, and 5 μm diameter (D_p)], and for each D_p three different flow rates ($\dot{Q}$ 150, 250, and 500 ml/s) were used. In all tests the same ($\dot{Q}$ was used for inspiration and expiration, and the inspiratory volume was maintained at 500 ml from FRC. For a given bolus delivery condition, at least five repeated measurements were made. For the purpose of comparison and validation, non bolus aerosols were also used in

a few subjects. The subject inhaled non-bolus aerosols from a 20 liter bag with a single breath maneuver (inhalation from FRC and exhalation to RV) that was the same maneuver used for bolus aerosols, and TDF values were obtained for several breaths. The same aerosols were then inhaled with a continuous breathing maneuver (inhalation from FRC and exhalation to FRC) for 1 min, and TDF was obtained breath by breath (Chong S. Kim & Gerrity, 1996).

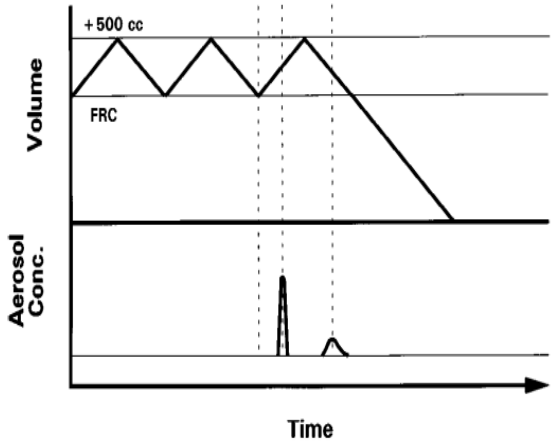

Figure 3.5: Schematic diagram depicting an inhalation maneuver for bolus aerosols. Inhalation started at functional residual capacity (FRC) with 500-ml tidal volume, and exhalation was to residual capacity. An aerosol bolus (45 ml half-width) was injected at prescribed time points during inspiration. Conc, concentration.

3.3 ICRP66 METHOD

The ICRP66 deposition model estimates regional deposition, i.e., deposition in each anatomical region of the respiratory tract. A semi empirical approach has been used to describe the regional deposition. Relative simple algebraic equations derived from experiments and theory are used for the deposition model.

Each breath is represented by a tidal flow of air that carries particles through each anatomical region which is represented by one or more filters in series. A filter j has two parameters, i.e., the volume v_j and the filtration efficiency $_j$, and $_j$ is the fraction of the tidal volume (denoted by V_t) which passes through the filter j. During inhalation, smaller and smaller fractions of the tidal volume pass through the filters in turn, which are determined by the cumulative volumes of the preceding filters. During exhalation, the same volume of air passes through the same filters as those during the inhalation. The filtration efficiency $_j$ of the filter j is the fraction of particles incident on the filter which is deposited. The filtration efficiency (which is equal to the deposition efficiency) for an anatomical region is given in the form

$$\eta = \exp(-aR^P) \tag{3.12}$$

Phase	Filter	Region	Aerodynamic regional deposition $\eta_{ae} = 1 - exp(-aR^p)$		
			a	R	p
Inspiration	1	ET_1	3×10^{-4}	$d_{ae}^2 V_n SF_t^3$	1
	2	ET_2	5.5×10^{-5}	$d_{ae}^2 V_n SF_t^3$	1.17
	3	BB	4.08×10^{-6}	$d_{ae}^2 V_n SF_t^{2.3}$	1.152
	4	bb	0.1147	$(0.056 + t_b^{1.5}) \times d_{ae}^t t_b^{-0.25}$	1.173
	5	AI	$0.146 \times SF_A^{0.98}$	$d_{ae}^2 t_A$	0.6495
Expiration	6	bb	0.1147	$(0.056 + t_b^{1.5}) \times d_{ae}^t t_b^{-0.25}$	1.173
	7	BB	4.08×10^{-6}	$d_{ae}^2 V_n SF_t^{2.3}$	1.152
	8	ET_2	5.5×10^{-5}	$d_{ae}^2 V_n SF_t^3$	1.17
	9	ET_1	3×10^{-4}	$d_{ae}^2 V_n SF_t^3$	1

Table 3.2: Recommended algebraic expressions for aerodynamic deposition

where a and p are parameters and R is a function of the particle diameter and flow rate. The function in Eq. (3.12) is given separately for thermodynamic and aerodynamic depositions

The ICRP66 model is also able to take into account the breathing habit since depositions in the nose and the mouth are different. Table 5 gives recommended parameters and functions for the regional aerodynamic deposition, and Table 6 gives the corresponding information for thermodynamic deposition, both for the fraction inhaled through the nose. Here ψ^{th} is the empirical correction factor to allow for enhancement of thermodynamic deposition caused by turbulent airflow in the first few generations of the T-B tree; and

$$V_D^{'}(BB) = V_D(BB)(1 + \frac{V_T}{FRC}) \tag{3.13}$$

and

$$V_D^{'}(bb) = V_D(bb)(1 + \frac{V_T}{FRC}) \tag{3.14}$$

t is the residence time of air in an anatomical region, and SF the respiratory are scaling factors from a Caucasian adult male to some other subjects. A scaling factor is defined as the ratio of a reference airway size in an adult Caucasian male to that in the subject. The characteristic airway size in the ET and BB regions is taken to be the diameter of the trachea. For the bb and AI regions, the characteristic airway sizes are the diameters of airways in the 9th and 16th generations, respectively. (Yu et al., 2006). The residence times are given by the following equations:

$$t_B = \frac{V_D(BB)}{V}(1 + \frac{0.55V_T}{FRC}) \tag{3.15}$$

$$t_b = \frac{V_D(bb)}{V}(1 + \frac{0.55V_T}{FRC}) \tag{3.16}$$

Phase	Filter	Region	Thermodynamic regional deposition ($\eta_{ae} = 1 - \exp(-aR^p)$)			Volumetric fraction
			a	R	p	
Inspiration	1	ET_1	18	$D(V \times SF_t)^{-1/4}$	1/2	1
	2	ET_2	15.1	$D(V \times SF_t)^{-1/4}$	0.538	1
	3	BB	$22.02 \times SF_t^{1.24}\psi_{th}$	Dt_B	0.6391	$1 - V_D(ET)/V_t$
	4	bb	$-76.8 + 167 \times SF_b^{0.65}$	Dt_b	0.5676	$1 - [V_D(ET) + V'_D(BB)]/V_T$
	5	AI	$170 + 103 \times SF_A^{2.13}$	Dt_A	0.6101	$1 - [V_D(ET) + V'_D(BB) + V'_D(bb)]/V_T$
Expiration	6	bb	$-76.8 + 167 \times SF_b^{0.65}$	Dt_b	0.5676	$1 - [V_D(ET) + V'_D(BB)]/V_T$
	7	BB	$22.02 \times SF_t^{1.24}\psi_{th}$	Dt_B	0.6391	$1 - V_D(ET)/V_t$
	8	ET_2	15.1	$D(V \times SF_t)^{-1/4}$	0.538	1
	9	ET_1	18	$D(V \times SF_t)^{-1/4}$	1/2	1

Table 3.3: Recommended algebraic expressions for thermodynamic deposition

$$t_A = \frac{V_T - V_D(ET) - [V_D(BB) + V_D(bb)](1 + \frac{0.55V_T}{FRC})}{V} \tag{3.17}$$

In this study Cheng′s method (in above section 3.1) used to generate and plot the following data and graph (fig.3.6).

3.4 Results and Discussion

The effect of flow rate ($\dot{Q}$) and particle size on extra-thoracic respiratory tract deposition efficiency (E_n) is displayed in Fig.3.6. The deposition efficiency for flow rate 7, 20 and 50 L/min is plotted as E_n function of normalized d_a^2 for each flow rate. The normalized d_a^2 refers to the d_a^2 value divided to the smallest value of d_a^2 ($1.00E^{-7}$).

Figure 3.6 shows The deposition efficiency is strongly size dependent, with the greatest deposition efficiency occurring for the largest particle size (for largest normalized d_a^2 number). Deposition efficiency around zero for normalized d_a^2 values from 0 to about 100 and gradually rise up and approaches to 1 at normalized d_a^2 values about 100000 and above. Deposition efficiency also flow rate dependent; in the rang of normalized d_a^2 values from 100 up to about 1000000 clearly seen that, as flow rate increase deposition also increases.

normalized d_a^2	d_a(m)	(d_a)^2	Q(Lit/min)	Diffusion coe	Impaction		
					E_n = 1-exp(-110Stk) at 7Lit/min	E_n = 1-exp(-110Stk) at 20Lit/min	E_n = 1-exp(-110Stk) at 50Lit/min
1	1.00E-07	1E-14	2.00E+01	7.80E-06	3.96E-06	1.13E-05	2.83E-05
4	2.00E-07	4E-14	2.00E+01	7.80E-06	1.58E-05	4.52E-05	1.13E-04
9	3.00E-07	9E-14	2.00E+01	7.80E-06	3.56E-05	1.02E-04	2.54E-04
16	4.00E-07	1.6E-13	2.00E+01	7.80E-06	6.33E-05	1.81E-04	4.52E-04
25	5.00E-07	2.5E-13	2.00E+01	7.80E-06	9.89E-05	2.83E-04	7.06E-04
36	6.00E-07	3.6E-13	2.00E+01	7.80E-06	1.42E-04	4.07E-04	1.02E-03
49	7.00E-07	4.9E-13	2.00E+01	7.80E-06	1.94E-04	5.54E-04	1.38E-03
64	8.00E-07	6.4E-13	2.00E+01	7.80E-06	2.53E-04	7.23E-04	1.81E-03
81	9.00E-07	8.1E-13	2.00E+01	7.80E-06	3.20E-04	9.15E-04	2.29E-03
100	1.00E-06	1E-12	2.00E+01	7.80E-06	3.96E-04	1.13E-03	2.82E-03
121	1.10E-06	1.21E-12	2.00E+01	7.80E-06	4.79E-04	1.37E-03	3.41E-03
144	1.20E-06	1.44E-12	2.00E+01	7.80E-06	5.70E-04	1.63E-03	4.06E-03
169	1.30E-06	1.69E-12	2.00E+01	7.80E-06	6.68E-04	1.91E-03	4.76E-03
196	1.40E-06	1.96E-12	2.00E+01	7.80E-06	7.75E-04	2.21E-03	5.52E-03
225	1.50E-06	2.25E-12	2.00E+01	7.80E-06	8.90E-04	2.54E-03	6.34E-03
256	1.60E-06	2.56E-12	2.00E+01	7.80E-06	1.01E-03	2.89E-03	7.21E-03
289	1.70E-06	2.89E-12	2.00E+01	7.80E-06	1.14E-03	3.26E-03	8.13E-03
324	1.80E-06	3.24E-12	2.00E+01	7.80E-06	1.28E-03	3.66E-03	9.11E-03
361	1.90E-06	3.61E-12	2.00E+01	7.80E-06	1.43E-03	4.07E-03	1.02E-02
400	2.00E-06	4E-12	2.00E+01	7.80E-06	1.58E-03	4.51E-03	1.12E-02
441	2.10E-06	4.41E-12	2.00E+01	7.80E-06	1.74E-03	4.97E-03	1.24E-02
484	2.20E-06	4.84E-12	2.00E+01	7.80E-06	1.91E-03	5.46E-03	1.36E-02
529	2.30E-06	5.29E-12	2.00E+01	7.80E-06	2.09E-03	5.96E-03	1.48E-02
576	2.40E-06	5.76E-12	2.00E+01	7.80E-06	2.28E-03	6.49E-03	1.61E-02
625	2.50E-06	6.25E-12	2.00E+01	7.80E-06	2.47E-03	7.04E-03	1.75E-02
676	2.60E-06	6.76E-12	2.00E+01	7.80E-06	2.67E-03	7.61E-03	1.89E-02
729	2.70E-06	7.29E-12	2.00E+01	7.80E-06	2.88E-03	8.21E-03	2.04E-02
784	2.80E-06	7.84E-12	2.00E+01	7.80E-06	3.10E-03	8.82E-03	2.19E-02
841	2.90E-06	8.41E-12	2.00E+01	7.80E-06	3.32E-03	9.46E-03	2.35E-02
900	3.00E-06	9E-12	2.00E+01	7.80E-06	3.55E-03	1.01E-02	2.51E-02
961	3.10E-06	9.61E-12	2.00E+01	7.80E-06	3.79E-03	1.08E-02	2.68E-02
1024	3.20E-06	1.024E-11	2.00E+01	7.80E-06	4.04E-03	1.15E-02	2.85E-02
1089	3.30E-06	1.089E-11	2.00E+01	7.80E-06	4.30E-03	1.22E-02	3.03E-02
1156	3.40E-06	1.156E-11	2.00E+01	7.80E-06	4.56E-03	1.30E-02	3.21E-02
1225	3.50E-06	1.225E-11	2.00E+01	7.80E-06	4.83E-03	1.38E-02	3.40E-02
1296	3.60E-06	1.296E-11	2.00E+01	7.80E-06	5.11E-03	1.45E-02	3.60E-02
1369	3.70E-06	1.369E-11	2.00E+01	7.80E-06	5.40E-03	1.54E-02	3.79E-02
1444	3.80E-06	1.444E-11	2.00E+01	7.80E-06	5.70E-03	1.62E-02	4.00E-02
1521	3.90E-06	1.521E-11	2.00E+01	7.80E-06	6.00E-03	1.70E-02	4.21E-02
1600	4.00E-06	1.6E-11	2.00E+01	7.80E-06	6.31E-03	1.79E-02	4.42E-02
1681	4.10E-06	1.681E-11	2.00E+01	7.80E-06	6.63E-03	1.88E-02	4.64E-02
1764	4.20E-06	1.764E-11	2.00E+01	7.80E-06	6.95E-03	1.97E-02	4.86E-02
1849	4.30E-06	1.849E-11	2.00E+01	7.80E-06	7.29E-03	2.07E-02	5.09E-02
1936	4.40E-06	1.936E-11	2.00E+01	7.80E-06	7.63E-03	2.16E-02	5.32E-02
2025	4.50E-06	2.025E-11	2.00E+01	7.80E-06	7.98E-03	2.26E-02	5.56E-02
2116	4.60E-06	2.116E-11	2.00E+01	7.80E-06	8.34E-03	2.36E-02	5.80E-02
2209	4.70E-06	2.209E-11	2.00E+01	7.80E-06	8.70E-03	2.47E-02	6.05E-02
2304	4.80E-06	2.304E-11	2.00E+01	7.80E-06	9.07E-03	2.57E-02	6.30E-02
2401	4.90E-06	2.401E-11	2.00E+01	7.80E-06	9.45E-03	2.68E-02	6.56E-02
2500	5.00E-06	2.5E-11	2.00E+01	7.80E-06	9.84E-03	2.79E-02	6.82E-02
2601	5.10E-06	2.601E-11	2.00E+01	7.80E-06	1.02E-02	2.90E-02	7.09E-02
2704	5.20E-06	2.704E-11	2.00E+01	7.80E-06	1.06E-02	3.01E-02	7.36E-02
2809	5.30E-06	2.809E-11	2.00E+01	7.80E-06	1.11E-02	3.13E-02	7.63E-02
2916	5.40E-06	2.916E-11	2.00E+01	7.80E-06	1.15E-02	3.24E-02	7.91E-02
3025	5.50E-06	3.025E-11	2.00E+01	7.80E-06	1.19E-02	3.36E-02	8.19E-02
3136	5.60E-06	3.136E-11	2.00E+01	7.80E-06	1.23E-02	3.48E-02	8.48E-02
3249	5.70E-06	3.249E-11	2.00E+01	7.80E-06	1.28E-02	3.61E-02	8.77E-02
3364	5.80E-06	3.364E-11	2.00E+01	7.80E-06	1.32E-02	3.73E-02	9.07E-02
3481	5.90E-06	3.481E-11	2.00E+01	7.80E-06	1.37E-02	3.86E-02	9.37E-02
3600	6.00E-06	3.6E-11	2.00E+01	7.80E-06	1.41E-02	3.99E-02	9.67E-02
3721	6.10E-06	3.721E-11	2.00E+01	7.80E-06	1.46E-02	4.12E-02	9.98E-02
3844	6.20E-06	3.844E-11	2.00E+01	7.80E-06	1.51E-02	4.25E-02	1.03E-01
3969	6.30E-06	3.969E-11	2.00E+01	7.80E-06	1.56E-02	4.39E-02	1.06E-01
4096	6.40E-06	4.096E-11	2.00E+01	7.80E-06	1.61E-02	4.52E-02	1.09E-01
4225	6.50E-06	4.225E-11	2.00E+01	7.80E-06	1.66E-02	4.66E-02	1.13E-01

normalized d_a^2	d_a(m)	(d_a)^2	Q(Lit/min)	Diffusion coe	Impaction		
					E_n = 1-exp(-110Stk) at 7Lit/min	E_n = 1-exp(-110Stk) at 20Lit/min	E_n = 1-exp(-110Stk) at 50Lit/min
435600	6.60E-05	4.356E-09	2.00E+01	7.80E-06	8.22E-01	9.93E-01	1.00E+00
436921	6.61E-05	4.36921E-09	2.00E+01	7.80E-06	8.22E-01	9.93E-01	1.00E+00
438244	6.62E-05	4.38244E-09	2.00E+01	7.80E-06	8.23E-01	9.93E-01	1.00E+00
439569	6.63E-05	4.39569E-09	2.00E+01	7.80E-06	8.24E-01	9.93E-01	1.00E+00
440896	6.64E-05	4.40896E-09	2.00E+01	7.80E-06	8.25E-01	9.93E-01	1.00E+00
442225	6.65E-05	4.42225E-09	2.00E+01	7.80E-06	8.26E-01	9.93E-01	1.00E+00
443556	6.66E-05	4.43556E-09	2.00E+01	7.80E-06	8.27E-01	9.93E-01	1.00E+00
444889	6.67E-05	4.44889E-09	2.00E+01	7.80E-06	8.28E-01	9.93E-01	1.00E+00
446224	6.68E-05	4.46224E-09	2.00E+01	7.80E-06	8.29E-01	9.94E-01	1.00E+00
447561	6.69E-05	4.47561E-09	2.00E+01	7.80E-06	8.30E-01	9.94E-01	1.00E+00
448900	6.70E-05	4.489E-09	2.00E+01	7.80E-06	8.31E-01	9.94E-01	1.00E+00
450241	6.71E-05	4.50241E-09	2.00E+01	7.80E-06	8.32E-01	9.94E-01	1.00E+00
451584	6.72E-05	4.51584E-09	2.00E+01	7.80E-06	8.32E-01	9.94E-01	1.00E+00
452929	6.73E-05	4.52929E-09	2.00E+01	7.80E-06	8.33E-01	9.94E-01	1.00E+00
454276	6.74E-05	4.54276E-09	2.00E+01	7.80E-06	8.34E-01	9.94E-01	1.00E+00
455625	6.75E-05	4.55625E-09	2.00E+01	7.80E-06	8.35E-01	9.94E-01	1.00E+00
456976	6.76E-05	4.56976E-09	2.00E+01	7.80E-06	8.36E-01	9.94E-01	1.00E+00
458329	6.77E-05	4.58329E-09	2.00E+01	7.80E-06	8.37E-01	9.94E-01	1.00E+00
459684	6.78E-05	4.59684E-09	2.00E+01	7.80E-06	8.38E-01	9.94E-01	1.00E+00
461041	6.79E-05	4.61041E-09	2.00E+01	7.80E-06	8.39E-01	9.95E-01	1.00E+00
462400	6.80E-05	4.624E-09	2.00E+01	7.80E-06	8.40E-01	9.95E-01	1.00E+00
463761	6.81E-05	4.63761E-09	2.00E+01	7.80E-06	8.40E-01	9.95E-01	1.00E+00
465124	6.82E-05	4.65124E-09	2.00E+01	7.80E-06	8.41E-01	9.95E-01	1.00E+00
466489	6.83E-05	4.66489E-09	2.00E+01	7.80E-06	8.42E-01	9.95E-01	1.00E+00
467856	6.84E-05	4.67856E-09	2.00E+01	7.80E-06	8.43E-01	9.95E-01	1.00E+00
469225	6.85E-05	4.69225E-09	2.00E+01	7.80E-06	8.44E-01	9.95E-01	1.00E+00
470596	6.86E-05	4.70596E-09	2.00E+01	7.80E-06	8.45E-01	9.95E-01	1.00E+00
471969	6.87E-05	4.71969E-09	2.00E+01	7.80E-06	8.45E-01	9.95E-01	1.00E+00
473344	6.88E-05	4.73344E-09	2.00E+01	7.80E-06	8.46E-01	9.95E-01	1.00E+00
474721	6.89E-05	4.74721E-09	2.00E+01	7.80E-06	8.47E-01	9.95E-01	1.00E+00
476100	6.90E-05	4.761E-09	2.00E+01	7.80E-06	8.48E-01	9.95E-01	1.00E+00
477481	6.91E-05	4.77481E-09	2.00E+01	7.80E-06	8.49E-01	9.95E-01	1.00E+00
478864	6.92E-05	4.78864E-09	2.00E+01	7.80E-06	8.50E-01	9.96E-01	1.00E+00
480249	6.93E-05	4.80249E-09	2.00E+01	7.80E-06	8.50E-01	9.96E-01	1.00E+00
481636	6.94E-05	4.81636E-09	2.00E+01	7.80E-06	8.51E-01	9.96E-01	1.00E+00
483025	6.95E-05	4.83025E-09	2.00E+01	7.80E-06	8.52E-01	9.96E-01	1.00E+00
484416	6.96E-05	4.84416E-09	2.00E+01	7.80E-06	8.53E-01	9.96E-01	1.00E+00
485809	6.97E-05	4.85809E-09	2.00E+01	7.80E-06	8.54E-01	9.96E-01	1.00E+00
487204	6.98E-05	4.87204E-09	2.00E+01	7.80E-06	8.55E-01	9.96E-01	1.00E+00
488601	6.99E-05	4.88601E-09	2.00E+01	7.80E-06	8.55E-01	9.96E-01	1.00E+00
490000	7.00E-05	4.9E-09	2.00E+01	7.80E-06	8.56E-01	9.96E-01	1.00E+00
491401	7.01E-05	4.91401E-09	2.00E+01	7.80E-06	8.57E-01	9.96E-01	1.00E+00
492804	7.02E-05	4.92804E-09	2.00E+01	7.80E-06	8.58E-01	9.96E-01	1.00E+00
494209	7.03E-05	4.94209E-09	2.00E+01	7.80E-06	8.58E-01	9.96E-01	1.00E+00
495616	7.04E-05	4.95616E-09	2.00E+01	7.80E-06	8.59E-01	9.96E-01	1.00E+00
497025	7.05E-05	4.97025E-09	2.00E+01	7.80E-06	8.60E-01	9.96E-01	1.00E+00
498436	7.06E-05	4.98436E-09	2.00E+01	7.80E-06	8.61E-01	9.96E-01	1.00E+00
499849	7.07E-05	4.99849E-09	2.00E+01	7.80E-06	8.62E-01	9.96E-01	1.00E+00
501264	7.08E-05	5.01264E-09	2.00E+01	7.80E-06	8.62E-01	9.97E-01	1.00E+00
502681	7.09E-05	5.02681E-09	2.00E+01	7.80E-06	8.63E-01	9.97E-01	1.00E+00
504100	7.10E-05	5.041E-09	2.00E+01	7.80E-06	8.64E-01	9.97E-01	1.00E+00
505521	7.11E-05	5.05521E-09	2.00E+01	7.80E-06	8.65E-01	9.97E-01	1.00E+00
506944	7.12E-05	5.06944E-09	2.00E+01	7.80E-06	8.65E-01	9.97E-01	1.00E+00
508369	7.13E-05	5.08369E-09	2.00E+01	7.80E-06	8.66E-01	9.97E-01	1.00E+00
509796	7.14E-05	5.09796E-09	2.00E+01	7.80E-06	8.67E-01	9.97E-01	1.00E+00
511225	7.15E-05	5.11225E-09	2.00E+01	7.80E-06	8.68E-01	9.97E-01	1.00E+00
512656	7.16E-05	5.12656E-09	2.00E+01	7.80E-06	8.68E-01	9.97E-01	1.00E+00
514089	7.17E-05	5.14089E-09	2.00E+01	7.80E-06	8.69E-01	9.97E-01	1.00E+00
515524	7.18E-05	5.15524E-09	2.00E+01	7.80E-06	8.70E-01	9.97E-01	1.00E+00
516961	7.19E-05	5.16961E-09	2.00E+01	7.80E-06	8.71E-01	9.97E-01	1.00E+00
518400	7.20E-05	5.184E-09	2.00E+01	7.80E-06	8.71E-01	9.97E-01	1.00E+00
519841	7.21E-05	5.19841E-09	2.00E+01	7.80E-06	8.72E-01	9.97E-01	1.00E+00
521284	7.22E-05	5.21284E-09	2.00E+01	7.80E-06	8.73E-01	9.97E-01	1.00E+00
522729	7.23E-05	5.22729E-09	2.00E+01	7.80E-06	8.74E-01	9.97E-01	1.00E+00
524176	7.24E-05	5.24176E-09	2.00E+01	7.80E-06	8.74E-01	9.97E-01	1.00E+00
525625	7.25E-05	5.25625E-09	2.00E+01	7.80E-06	8.75E-01	9.97E-01	1.00E+00

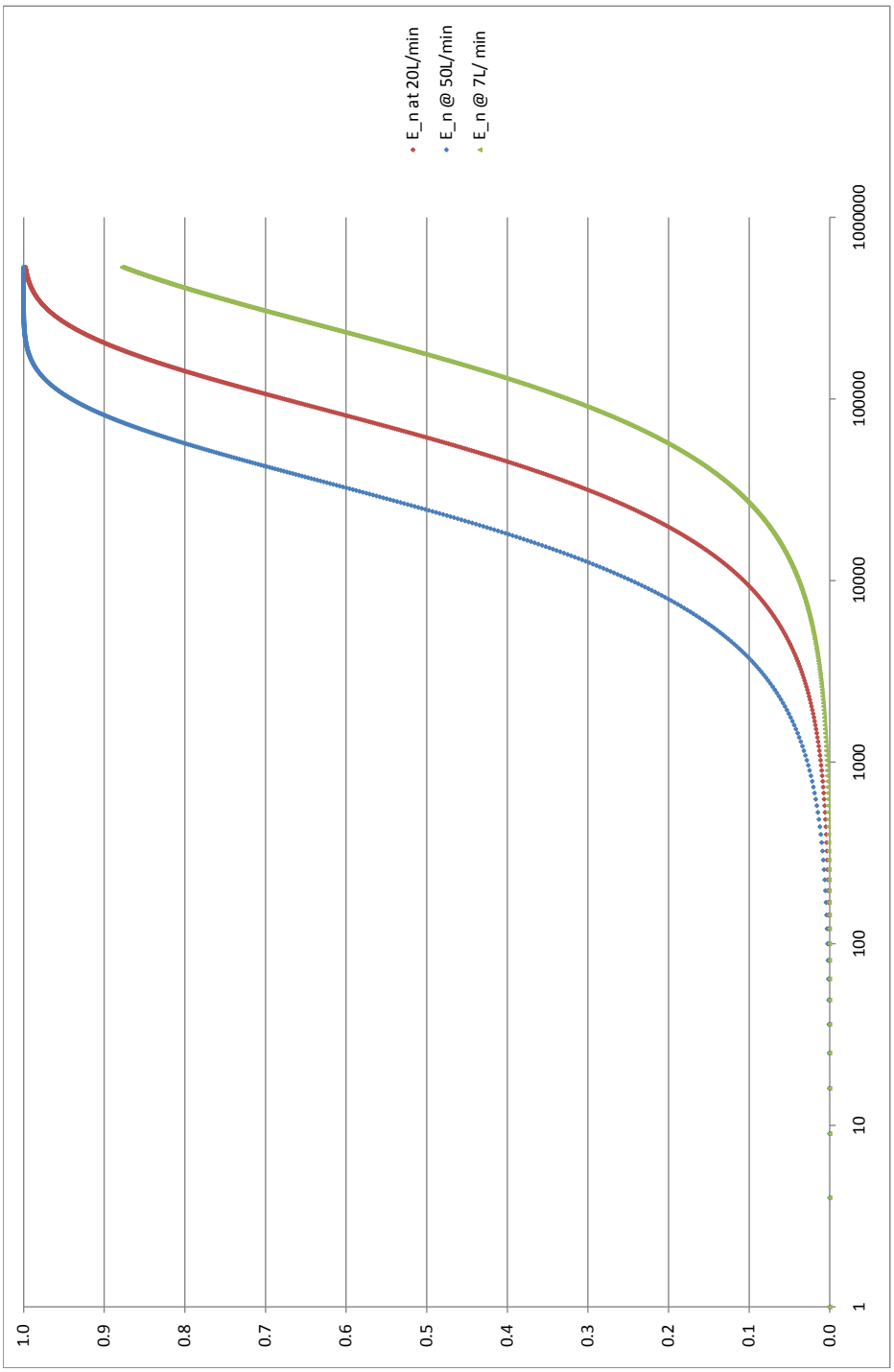

Figure 3.6: Dependence of Deposition Efficiency for different flow rates

CHAPTER 4
CONCLUSION AND RECOMMENDATION

4.1 CONCLUSIONS

Aerosols are mixed in air and they enter into the human lung during inhalation. A fraction of them is deposited in the lung. There are two groups of deposition processes, i.e., thermodynamic and aerodynamic deposition. The former is characteristic for small-diameter particles and is often called diffusion or Brownian deposition. This type of deposition is caused by the random movement of the aerosols in the air stream. When the aerosols "touch" the wall of the airway tube, they can stay in that position. Aerodynamic deposition is more important for larger particles and there are two types of processes belonging to this group. The first one is "impactional" or inertial deposition. This deposition process takes place when the air stream changes the direction; some of the airborne aerosols with larger mass cannot adjust their directions of movement sufficiently quickly because of their inertia, and impact onto the wall of the airway tube. The second aerodynamic deposition process is gravitational sedimentation of aerosols. There are also other less important deposition processes like interception, which is important for fibers, etc.

The deposition efficiency of aerosols in the size range (0.1 μm to 72 μ is shown in figure 3.6

From figure 3.6 it is clear that the deposition in the nasal part of the extra-thoracic region is dominated by the impaction process. For high values of aerosol diameter, and faster breathing rates the deposition efficiency gets higher. i.e. :

- more than 50% of aerosols of diameter $> 0.42\mu$ m are deposited in the extra-thoracic region at breathing rate of 7 L/min.
- more than 50% of aerosols of diameter $> 0.25\mu$ m are deposited in the extra-thoracic region at breathing rate of 20 L/min.
- more than 50% of aerosols of diameter $> 0.15\mu$ m are deposited in the extra-thoracic region at breathing rate of 50 L/min.

These observations agree with ICRP 66 lung model that predicts the dominance of imitational process in higher aerosol sizes.

Experimental works shown in Figures 3.1 and 3.2 also indicate similar variation. When it comes to the mathematical model discussed in this work more precise experimental fit can be obtained by introducing adjustment parameters.

4.1.1 Recommendations

- the work can be extended to other parts of the respiratory tract by taking into account:
  - different geometric sizes of the respiratory tract for people of different physiology
  - the clearing mechanism of aerosols
- identification of the deposition efficiency of aerosols is a forerunner of exact dose determination in different parts of the respiratory tract. Therefore this work can gradually develop to a model of dose dtermination

Bibliography

Allan L. Coates, M. C. (2008). Guiding aerosol deposition in the lung. *The new England journal of medicine*.

Bemenet Alemayehu (2006). Measuring radon concentration using filtered air samples. *Addis Ababa Ethiopia*.

Boecker, B. B. (1995). Comparison of old and new icrp models for respiratory tract dosimetry. Report NM 87185, Inhalation Toxicology Research Institute.

Cember, H. & Johnson, T. E. (2009). *Introduction to Health Physics* (FOURTH EDITION ed.). New York Chicago San Francisco Lisbon London Madrid Mexico City Milan New Delhi San Juan Seoul Singapore Sydney Toronto: McGraw-Hill Companies.

Chantal Darquenne, M. P. J. B. W. & Prisk, G. K. (1997). Effect of microgravity and hypergravity on deposition of 0.5- to 3-Îijm-diameter aerosol in the human lung. *J Appl Physiol*, *83*, 2029–2036.

Cheng, Y. S. (2003). Aerosol deposition in the extrathoracic region. *Aerosol Science and Technology*, *25*(2), 659–671.

Cheung, T. & Yu, K. (2004). Bronchial dosimeters for radon progeny for chinese males and females. *Journal of Environmental Radioactivity*, *71*, 215–224.

Chong S. Kim, S. C. H. P. D. & Gerrity, T. R. (1996). Assessment of regional deposition of inhaled particles in human lungs by serial bolus delivery method. *Journal of Applied Physiology*, *81*, 2203–2213.

Craven, S. A. & Smit, B. J. (2006). Radon in caves clinical aspects. *International Journal of Speleology*, *2*(35), 93 – 101.

ERNBO, H. (2006). Minimum detectable amount of radon progeny in outdoor air. *Stockholm, Sweden*.

George, A. C. (2008). World history of radon research and measurement from the early 1900's to today. *NATURAL RADIATION ENVIRONMENT*, *1034*, 20–33.

George, A. C. & Knutson, E. O. (1992). Radon progeny deposition in the nasal and tracheobronchial regions of the respiratory tract. *Journal of Radiation Protraction Dosimetry*, *Vol.45*(No Âij).

GLOBE (2002). *Aerosol Protocol*.

Hawarynski, M. & Domanski, T. (1982). Theory of radon daughter products interaction with water vapor in the ambient air. *Proc of the 2nd Sp Symp. On Nat Rad Envt,Bombay India*, 592–597.

Hayes, K. K. (1991). The production of sulfate particles through the radiolytic oxidation of sulfur dioxide. Master's thesis, Addis Ababa University School of Graduate Studies, Ethiopia, Department of Chemistry Clarkson University.

Heyder, J. (2004). Deposition of inhaled particles in the human respiratory tract and consequences for regional targeting in respiratory drug delivery. *National Research Center for Environment and Health*, *1*, 315–320.

Hobbs, P. V. (Ed.). (1993). *Aerosol-cloud climate Interaction*, volume 54 of *Tracts In Modern Physics*. Academic Press Limited.

Hofmann, W. (1998). Overview of radon lung dosimetry. *Radiation Protection Dosimetry*, *Vol. 79*(1–4), 229–236.

Hopke, P. K., Ramamurthi, M., & Knutson, E. O. (1990). A measurement system for rn decay product lung deposition based on respiratory models. *Jouran of Health Physics*, *58*(3), 291–295.

ICRP (2009). International commission on radiological protection statement on radon. Report ICRP Ref 00/902/09, ICRP.

Johnson, N. F., Newton, G. J., Thomassen, D. G., Guilmette, R. A., & Yeh, H. C. (1991). Risks from radon progenyexposure. *Inhalation Toxicology Research Institute, Lovelace Biomedical and Environmental Research Institute, Inc., Albuquerque, New Mexico*, *31*, 569–601.

Junge, C. (1963). *Air Chemistry and Radioactivity*. Academic press.

Kendall, G. M. & Smith, T. J. (2002). Doses to organs and tissues from radon and its decay products. *RADIOLOGICAL PROTECTION*.

Lewis, R. K. (2006). A history of radon- 1470 to 1984. *Environmental Protection Bureau of Radiation Protection*.

Papastefanou, C. (2008). *RADIOACTIVE AEROSOLS* (First edition ed.)., volume Volume 12. Elseviers Science and Technology Rights Department in Oxford, UK: Elsevier publications.

Porstendörfer, J. & Mercer, T. (1978). Influence of nuclei concentration and humidity upon attachment rate of atoms in the atmosphere. *Atmos Envr*, *12*, 2223.

Sarangapani, R. & Wexler, A. S. (2000). The role of dispersion in particle deposition in human airways. *Jouran of Toxicological Sciences*, *54*, 229–236.

Stranden, E. & Berteig, L. (1982). Radon daughter equilibrium and unattached fractions in mine atmospheres. *Health Physics*, *42*(2).

Stuart, B. O. (1984). Deposition and clearance of inhaled particles. *Environmental Health Perspective*, *55*, 369–390.

Tsega Berhane Teklu (2007). In door and out door variation of radon concentration. Master's thesis, Addis Ababa University School of Graduate Studies, Ethiopia.

Turner, J. E. (1995). *Atom Radiation and Radiation Protection* (2nd ed.)., volume 54. JOHON WILEY SON .INC,CANADA.

UNSCEAR (2006). Effects of ionizing radiation. Report to the General Assembly Volume 1, United Nations Scientific Committee on the Effects of Atomic Radiation (UNSCEAR), New York.

Yang, X. & Wenig, M. (2009). Study of columnar aerosol size distribution in hong kong. *Atmospheric Chemistry and Physics*, *9*, 6175–6189.

Yeh, H.-C., Cuddihy, R. G., Phalen, R. F., & Chang, I.-Y. (1996). Comparisons of calculated respiratory tract deposition of particles based on the proposed NCRP model and the new ICRP66 model. *Aerosol Science and Technology*, *25*(2), 134–140.

Yu, K., Lau, B., & Nikezic, D. (2006). Assessment of environmental radon hazard using human respiratory tract models. *Jouran of Hazardos Materials*, *132*, 98–110.

Yu, K., Laua, B., Guan, Z., Lo, T., & Young, E. (2001). Bronchial rn dose survey for residences. *Journal of Environmental Radioactivity*, *54*, 221–229.

DECLARATION

I the under signed declare that the thesis is my original work, has not been presented for a degree in any other university and that all sources of material used for the thesis have been duly acknowledged.

Name: _____

Signature: _____

This Thesis has been submitted for examination with my approval as university advisor.

Name: _____

Signature: _____